The Regeneration of Granular Activated Carbon

Using Hydrothermal Technology

by

Michael David Sufnarski, B.S.

Thesis

Presented to the Faculty of the Graduate School of

The University of Texas at Austin

in Partial Fulfillment

of the Requirements

for the Degree of

Master of Science in Engineering

The University of Texas at Austin
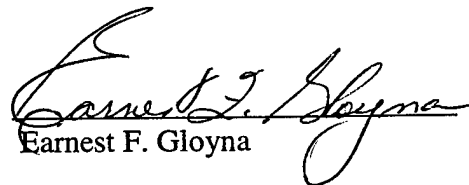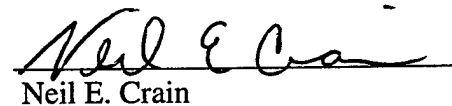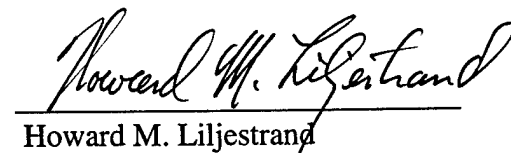
May 1999

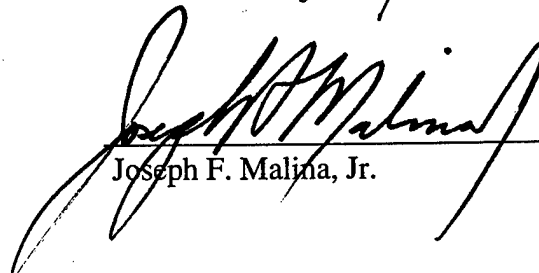The Regeneration of Granular Activated Carbon

Using Hydrothermal Technology

APPROVED BY

SUPERVISING COMMITTEE:

Supervisor:

Earnest F. Gloyna

Neil E. Crain

Howard M. Liljestrand

Joseph F. Malina, Jr.

ACKNOWLEDGMENTS

ABSTRACT

The Regeneration of Granular Activated Carbon

Using Hydrothermal Technology

by

Michael David Sufnarski, M.S.E.

The University of Texas at Austin, 1999

Supervisor: Earnest F. Gloyna

The economic feasibility of using granular activated carbon (GAC) to remove organic contaminants from industrial and municipal wastewater is contingent upon its reuse during multiple adsorption-regeneration cycles (Van Vliet, 1991). The most common process for the regeneration of GAC is the thermal method. Drawbacks associated with thermal regeneration include a 5-10% loss of carbon due to oxidation and attrition, a decrease in adsorption capacity, and high energy costs.

The purpose of this study was to investigate the regeneration of GAC using hydrothermal technology. Phenol contaminated and non-contaminated GAC samples were regenerated using supercritical water (411 °C and 26.2 MPa) with dissolved oxygen concentrations of 0 mg/L, 5 mg/L, and 100 mg/L. For comparative purposes, GAC was regenerated using subcritical water (300 °C and 12.4 MPa) with a dissolved oxygen concentration of 5 mg/L. Regenerated GAC samples were evaluated in terms of adsorption capacity, BET surface area, pore volume, and average pore size.

After four adsorption-regeneration cycles, using supercritical water (SCW) regeneration, the average adsorption capacity of regenerated GAC was found to

be 90% of that of virgin GAC. Although a slightly higher adsorption capacity was achieved for regeneration with degassed water, the overall impact of dissolved oxygen was insignificant. The high adsorption capacity achieved for SCW was not observed for subcritical water regeneration. After four adsorption-regeneration cycles, only 67% of the original adsorption capacity was restored. The better results observed for SCW, as compared to subcritical water, were related to two factors. First, the higher regeneration temperatures of SCW resulted in increased thermal desorption. Second, the increased solubility of organic compounds and enhanced mass transfer rates in SCW resulted in a more efficient extraction process.

TABLE OF CONTENTS

LIST OF TABLES

LIST OF FIGURES

1.0 INTRODUCTION

There are economic and environmental incentives to regenerate products derived from waste treatment processes. One such product is granular activated carbon (GAC), a solid adsorbent used to remove a wide range of organic compounds from industrial and municipal wastewater. After reaching its uptake capacity, GAC must either be disposed of and replaced with fresh carbon or be regenerated. The relative high initial cost of activated carbon, and the fact that disposal of spent adsorbents via landfills or incineration adds pollutants to the environment, mandates serious consideration of carbon regeneration.

The most common regeneration technique is thermal regeneration. In this method, organic substances sorbed onto GAC are oxidized by heating spent carbon to a temperature between 800-1000 °C in a furnace. Drawbacks associated with thermal regeneration include a 5-10% loss of carbon due to oxidation and attrition, a decrease in adsorption capacity, and high-energy costs associated with the required high temperatures (Magne and Walker, 1986; Hutchins, 1975).

Over the past two decades, several studies have focused on developing new cost-effective and efficient regeneration methods. For example, one class of studies reported the effectiveness of regenerating GAC by wet air oxidation (WAO). Using this technology, desorption and oxidative destruction of organic contaminants took place in a single process. Mundale et al. (1991) investigated the regeneration by WAO of GAC loaded with phenol and reported carbon losses ranging from 5-10% at a temperature of 185 °C and a pressure of 0.5 MPa. However, carbon losses were less at a temperature of 150 °C and the same pressure. A loss of adsorption capacity was attributed to surface oxidation and carbon-oxygen complexes on the surface of the carbon.

Another carbon regeneration study involved the thermal desorption of contaminants from spent carbon by high-temperature water (300 °C and 12.2

MPa) (Salvador and Sanchez, 1996). The procedure proved effective for removing phenols, textile dyes and pesticides. For some forms of GAC, original adsorption capacity was recovered during each of seven regeneration cycles.

Other researchers reported on the regeneration of activated carbon with supercritical CO_2 (Modell et al., 1980; Tan and Liou, 1988). The effectiveness of regeneration by supercritical CO_2 was dependent upon the physical and chemical bonding characteristics of the adsorbed compound. GAC exhausted with phenol and alacholar both exhibited a loss of adsorption capacity after one regeneration cycle; however, no additional losses were observed during successive regeneration cycles. GAC exhausted with acetic acid exhibited a complete recovery of adsorption capacity during each of seven regeneration cycles. The advantages of supercritical CO_2 extraction technology as compared to conventional thermal methods include lower energy requirements and lower carbon losses.

While supercritical water oxidation (SCWO) is a proven concept for the destruction of organic wastes, related studies have shown its potential for regeneration of inorganic absorbents contaminated with organic substances (Salvador et al., 1996). In general, water at ambient conditions is an ineffective regenerant of activated carbon due to the relatively low solubility of organic compounds (Pahl et al., 1973). However, with the increased solubility of organic compounds in supercritical water (SCW), there is the potential that contaminants can be effectively desorbed without altering the physical characteristics of the adsorbent.

1.1 Objective

The purpose of this study was to utilize hydrothermal technology to regenerate contaminated granular activated carbon (GAC). Specifically, the objective was to

evaluate regenerated GAC samples in terms of adsorption capacity, BET surface area, pore volume, and average pore size.

1.2 Scope

A column of adsorbent was subjected to a series of adsorption and regeneration cycles using a bench-scale, hydrothermal, adsorption-regeneration system. The selected adsorbent was NORIT Row 0.8 Supra GAC. Phenol was used as the adsorbate. Adsorption conditions were constant for all experiments. Regeneration experiments were conducted using supercritical water (411 $^{\circ}$C and 26.2 MPa) with dissolved oxygen concentrations of 0 mg/L, 5 mg/L, and 100 mg/L. Contaminated GAC was also regenerated using subcritical water (300 $^{\circ}$C and 12.4 MPa) with a dissolved oxygen concentration of 5 mg/L. For comparative purposes, non-contaminated GAC was subjected to identical regeneration conditions.

Adsorption capacities of virgin and regenerated GAC were calculated using a packed-bed column. Surface area and pore size distributions were determined by BET analysis. Physical changes in the activated carbon surface after regeneration were viewed with a scanning electron microscope (SEM). All feed concentrations and liquid samples were analyzed for total organic carbon (TOC). Adsorption breakthrough and regeneration wash-out curves were developed for selected experiments.

1.3 Rationale

The unique characteristics of SCW may represent the ideal medium for desorbing organic contaminants while preserving the physical characteristics of activated carbon. SCW regeneration should combine the effects of both thermal regeneration and chemical regeneration in a single non-oxidizing environment. The relatively high temperatures should result in thermal desorption while the

3

increased solubility of organic compounds and enhanced mass transfer rates of SCW should produce an effective extraction process. As compared to regeneration with supercritical CO_2, the smaller sized water molecule should penetrate deeper into the pores of activated carbon. Additional advantages of using SCW to regenerate GAC likely include reduced energy requirements and lower carbon losses than thermal regeneration since it operates at significantly lower temperatures than an industrial regeneration furnace.

The impact of dissolved oxygen in SCW during the regeneration of spent GAC is important from an economic viewpoint. Degassing operations to eliminate dissolved oxygen prior to regeneration with SCW potentially represent a significant process cost. Ideally, degassing is not necessary and the regeneration process can be used in conjunction with SCWO. Although the concentrations of dissolved oxygen used in this study are not high enough to oxidize the desorbed phenol, the results will help guide further studies. If dissolved oxygen is found to have little or no negative impact on the regeneration of GAC, it may be possible to regenerate the GAC and oxidize the desorbed contaminants in a single reactor. However, should degassing be required, a two-stage process would be necessary. Regeneration of spent GAC and destruction of desorbed organic contaminants would occur as two independent processes, most likely in separate reactors. In either scenario, the adsorbent is recycled and there is no discharge of hazardous contaminants to the environment.

2.0 LITERATURE EVALUATION

Relevant topics of this literature evaluation include the production, classification, industrial applications, and regeneration of granular activated carbon (GAC). An overview of solid-liquid phase adsorption is included. Emphasis is placed on current regeneration methods and the properties of supercritical water (SCW) as they relate to the regeneration of GAC. At the time of this study, there is an insignificant quantity of published literature pertaining to the regeneration of GAC using SCW.

2.1 Production of Granular Activated Carbon

The term "activated carbon" (AC) defines a group of carbonaceous materials with a highly developed internal surface area and porosity that possess a large capacity for adsorbing contaminants from liquids and gases (Patrick, 1995). Activated carbon materials in the form of granules, extrudates, or powders can be produced from virtually any carbonaceous material. Production of AC products can be accomplished by either thermal or chemical methods. Common feedstocks include peat, coal, wood, lignite, and nut shells. Criteria for selecting a feedstock include potential for producing high-quality carbon, availability, cost, storage life, and workability. The properties of the final AC product are a function of both the feedstock and the preparation procedure.

2.1.1 Thermal Processing

Figure 2.1 depicts a generalized process flow diagram of the thermal method of activated carbon production. Although not all of the steps are inclusive to every type of carbon, the two steps that always apply to thermal processing are carbonization and activation. Carbonization produces the initial porous structure of the carbon while activation converts the carbonized by-product to an adsorbent

5
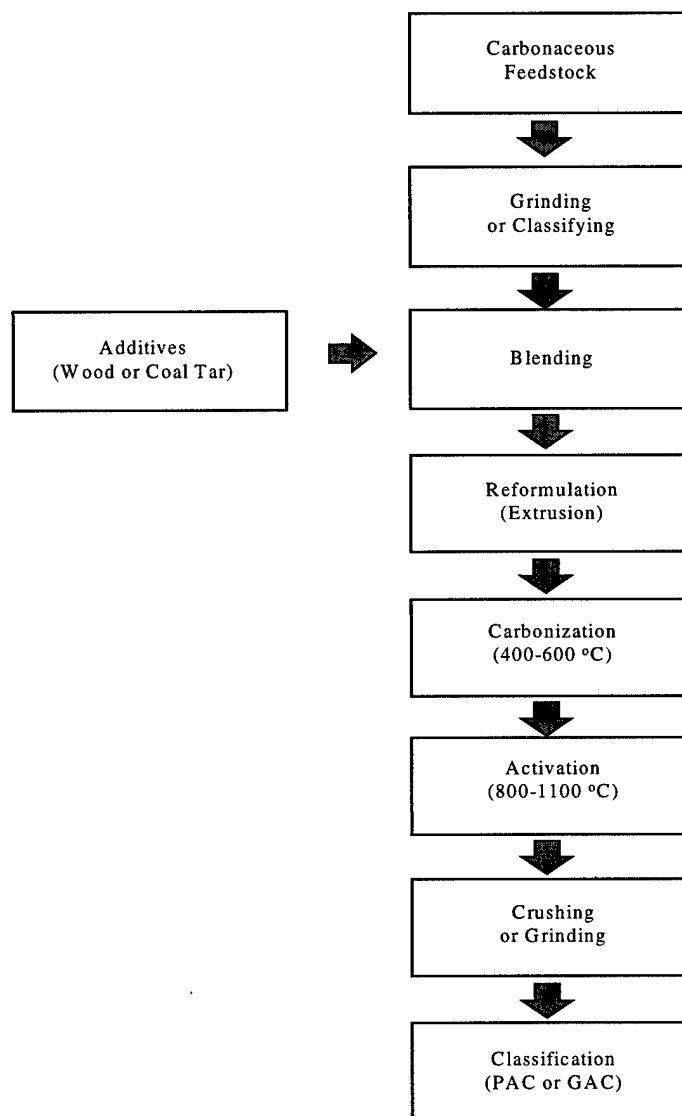
Figure 2.1 Thermal Processing Method of Activated Carbon Production (Patrick, 1995).

6

with a highly developed surface area and high porosity.

The preparation of the raw material prior to carbonization depends on the initial feedstock and the desired end product. Hard raw materials such as nut shells and anthracite coal are carbonized in lump form. Soft materials such as peat are ground and blended with a binding agent, usually wood or coal tar, to produce a homogeneous paste. The paste is then extruded from a steel die (1.5-6 mm diameter) and cut into uniform pieces prior to carbonization (Patrick, 1995).

During carbonization, the prepared raw material is gradually heated to 400-600 °C (Smisek and Cerny, 1970). Initially, as the temperature of the raw material reaches 200 °C, excess water and volatile organic compounds are released. Above this temperature, pyrolytic decomposition degrades the raw material and carbon dioxide, carbon monoxide, acetic acid, methanol, and tar are produced. Carbonization is completed between 400-600 °C when the base material is converted to elemental carbon as non-carbon elements (oxygen, nitrogen, and hydrogen) are released as gases. During the carbonization process, residual carbon atoms group themselves into organized crystallographic formations known as elementary crystallites (Smisek and Cerny, 1970). The arrangement of these formations is irregular which creates void spaces that may be blocked with pyrolytic residue. As a result, the carbonized product exhibits a small adsorption capacity with a surface area of only several m^2/g (Jankowska et al., 1991).

The carbon is "activated" in a two-stage process by introducing oxidizing agents, usually steam, air, or carbon dioxide at temperatures between 800-1100 °C (Bansal, et al., 1988). During the first stage, the clogged voids between the crystallites are opened exposing the surface to the activating agent. During the second stage, the existing voids are widened and new voids are created as the oxidizing agent attacks the surface of the crystallites and creates a series of fissures and cracks called pores. The final activated carbon product normally has a surface area of 500-1500 m^2/g (Wigmans, 1989).

7

The extent of oxidation depends on the development of the pores during carbonization and the type of activating agent. A measure of the extent of oxidation is termed burn-off, which is the difference in weight between the carbonized by-product and the activated product. When conditions are optimized in terms of oxidizing gas, temperature, flow rate and pressure, an acceptable compromise exists between 'selective' burn-off of carbon atoms and 'external' burn-off, which is the removal of carbon without an increase in porosity (Patrick, 1995). Oxidation of chars with no pore structure result in only a burn-off of the surface of the carbon.

Reaction rates also influence the development of porosity. In general, lower reaction rates result in greater porosity. Activation with steam and carbon dioxide (CO_2) involve the following reactions (Patrick, 1995):

$$C + H_2O \rightarrow CO + H_2 \qquad (\Delta H = + 130 \text{ kJ mol}^{-1})$$

and

$$C + CO_2 \rightarrow 2CO \qquad (\Delta H = + 159 \text{ kJ mol}^{-1})$$

Both reactions are endothermic and require external heating to maintain the reaction temperature. As a result, the reactions tend to be uniform and easy to control. However, steam is the preferred activating gas because a water molecule has smaller dimensions than a carbon dioxide molecule that results in faster and deeper diffusion into the porous network (Patrick, 1995). The larger carbon dioxide molecules tend to promote external oxidation and the development of larger pores than activation with steam (Bansal et al., 1988).

Activation with oxygen involves the following reactions (Patrick, 1995):

$$C + O_2 \rightarrow CO_2 \qquad (\Delta H = - 387 \text{ kJ mol}^{-1})$$

and

$$2C + O_2 \rightarrow 2CO \qquad (\Delta H = - 226 \text{ kJ mol}^{-1})$$

Both reactions are exothermic, so the rate and extent of reaction cannot be controlled by varying the heat supplied to the activation process. Additionally, since oxygen is an aggressive oxidant, excessive surface burn-off often results in a loss of carbon. As a result, activation with oxygen is rarely used (Smisek and Cerny, 1970).

2.1.2 Chemical Activation

In chemical activation, non-carbonized base materials are mixed with dehydrating agents such as phosphoric acid, sulfuric acid, or zinc chloride at temperatures in the range of 500–900 °C. This process is almost exclusively reserved for wood based materials, normally peat or sawdust, since the relevant reactions of the dehydrating agents require cellulosic structures (Smisek and Cerny, 1970).

Initially, the base material is heated and mixed with a concentrated dehydrating agent to degrade cellulose. The resulting material is then heated in a rotary kiln in the absence of air where pyrolytic decomposition occurs. The carbonized product is cooled and the activating agent is removed via washing in order to expose the porous structure. Although this process results in small uniform pores with high adsorption capacity, the carbon is usually contaminated with the dehydrating agent. As a result, thermal processing is the preferred production method.

2.2 Classification of Activated Carbon

Once formed, AC is classified into two groups: granular activated carbon (GAC) and powdered activated carbon (PAC). The size of GAC normally ranges from 40 mesh (0.425 mm) to 8 mesh (2.36 mm) while the size of PAC is smaller than 325 mesh (0.025 mm) (Droste, 1997).

GAC can either be crushed or pressed. Crushed carbons are prepared by

9

activating a lump material and crushing it to an appropriate size. Pressed carbons or extruded carbons are produced as uniform cylindrical shapes prior to carbonization. In general, GAC is characterized by relatively small pore diameters and large internal surface areas.

PAC is commonly produced by activating a lump material or lumps of paste prepared by mixing sawdust with zinc chloride, and subsequently grinding the activated product. Depending on the method of grinding, the shape of the particles may differ which affects its adsorptive properties. In general, PAC is characterized by relatively large pore diameters and small internal surface areas.

2.3 Adsorption

Adsorption is the process by which molecules present in one phase tend to condense and concentrate on the surface of another phase (Sawyer et al., 1994). Although the adsorption process occurs at the gas-solid, gas-liquid, solid-solid, liquid-liquid, and liquid-solid interfaces, this discussion focuses on the liquid-solid interface that applies to the use of GAC in water and wastewater treatment. The liquid being adsorbed is called as the adsorbate while the adsorbing solid is called the adsorbent. When adsorbed molecules are freed from the surface into the liquid phase, the process is called desorption.

Adsorption can either be physical (physiosorption) or chemical (chemisorption) depending on the forces responsible for adherence of the adsorbate onto the adsorbent. Although difficult to differentiate between the two sorptive mechanisms, a generally accepted criterion is based on adsorption energy. Typically, physical adsorption involves energies ranging from 4-30 kJ mol^{-1} and chemical adsorption involves energies ranging from 40-400 kJ mol^{-1} (Jankowska et al., 1991).

Physiosorption occurs when weak electrical attractive forces, known as van der Walls' forces, cause the adsorbate molecules to become physically attached to the

10

adsorbent molecules. This type of adsorption normally results in multiple layers of adsorbed molecules on the surface of the adsorbent. The number of layers formed is proportional to the concentration of the adsorbate. In general, physical adsorption is reversible by increasing the temperature or decreasing the concentration of the adsorbate.

Chemical adsorption is much stronger since it is caused by a chemical reaction between the adsorbed molecule and the adsorbent that results in the transfer and sharing of electrons. Normally, the adsorbate forms a surface that is only a single layer thick and the adsorbed molecule is not allowed to move from one site to another. The adsorbent is exhausted or spent when a single layer of molecules covers its entire surface. The amount of energy required to break the bonds of chemisorption is dependent upon the strength of the chemical bond between the adsorbate and the adsorbent.

2.4 Carbon Properties Related to Adsorption

The characterization of GAC is based on several physical and chemical properties including surface area, pore size distribution, and ability to adsorb selected substances.

The large surface area of activated carbon is related to its porous structure. The pores have been classified by the International Union of Pure and Applied Chemistry (IUPAC) into micropores (diameters < 20 angstroms), mesopores (diameter between 20 and 500 angstroms, and macropores (diameters > 500 angstroms) (Bansal et al., 1988).

Each of the pores has its specific function during adsorption. Most important are the micropores, located deep under the surface that provide the largest surface area. Micropores provide the adsorptive sites for small molecules and are also the primary sites of chemisorption since they are sites with the highest adsorption energies (Wigmans, 1989). The mesopores, also known as transitional pores,

serve two functions. Besides their significant contribution to the adsorption of larger molecules, they act as transport arteries to the micropores. The large macropores do not contribute greatly to surface area and the amount of material adsorbed in them is insignificant. Their main function is to allow adsorbate molecules to pass rapidly to the deeper pores.

The suitability of GAC to a specific application depends on the ratio in which the different pore sizes are present. Pore distribution varies greatly and is related to the base material and method of activation (Wigmans, 1989). For removal of large molecules, the GAC requires a large surface area or pore volume present as mesopores since the smaller micropores are inaccessible. For removal of small molecules, the GAC requires a large surface area or pore volume present as micropores.

In general, pore volume created during activation increases with increasing burn-off. According to Smisek and Cerny (1970), a burn-off of less than 50% produces a microporous carbon, a burn-off greater than 75% produces a macroporous carbon, and a burn-off between 50-75% produces a well-mixed porous carbon.

The total surface area and pore volume of activated carbon is normally estimated by the adsorption of nitrogen gas by the Brunauer-Emmett-Teller (BET) method (Smisek and Cerny, 1970). The distribution of pores of different diameters is measured by determining the amount of nitrogen adsorbed and desorbed under varying pressures. However, since nitrogen is a very small molecule, the BET method is not the best measure of overall quality because it does not include surface area available for larger molecules (Bansal, et al., 1988).

A method for determining the area available for larger molecules is by measuring the amount of adsorbate of a given molecular size (iodine, molasses, or methylene blue) that is removed from solution. For example, the amount of iodine adsorbed from solution is proportional to the surface area contributed by

12

pores having diameters greater than 10 angstroms (Cooney, 1999). Similarly, the adsorption of methylene blue is proportional to the surface area of pores with diameters greater than 15 angstroms (Cooney, 1999).

Adsorption rate is closely related to accessibility of pore structure and the dimensions of the adsorbate. The adsorption of organic compounds in solution by GAC is a four-step process. First, there is bulk diffusion of the adsorbate through the liquid to the boundary layer around the carbon particle. Second, dissolved organic compounds pass through the boundary layer to the exterior of the carbon particle. The organic compounds then diffuse into the pores of the GAC before they are finally adsorbed on the interior surfaces of the pores.

Particle size is generally considered to affect adsorption rate, but not adsorption capacity (U.S. EPA, 1973). The external surface area represents only a small percent of the total surface area of an activated carbon particle. Since adsorption capacity is related to total surface area, a given mass of carbon gains little adsorption capacity by being crushed to a smaller size.

Other factors that affect adsorption rate and capacity from the liquid phase include the size of the adsorbate molecules, the pH, the concentration of adsorbate in solution, the residence time of the system, and the chemical nature of the carbon surface.

The chemical nature or polarity varies with carbon type and influences the attractive forces between the molecules. In general, GAC surfaces are non-polar, making adsorption of inorganic electrolytes difficult and the adsorption of organic molecules easy (Cheremisinoff and Morresi, 1978). During activation, carbon-oxygen complexes form as oxygen is picked up by the carbon from the raw material or from the oxidizing gases (CO_2, O_2, and steam) used for activation. These complexes are usually classified as either basic or acidic. Depending on the temperature of the activation process, different complexes are formed that affect the adsorption characteristics of the activated carbon. Carbons activated at

13

low temperatures (200-500 °C) develop acidic surface oxides that include phenolic hydroxyl, carboxyl, and lactic groups (Cookson, 1978). Carboxyl groups make the surface polar and decrease the adsorption of non-polar compounds while hydroxyl groups tend to discourage the adsorption of aromatic compounds. Carbons activated at higher temperatures (800–1000 °C) form basic oxides that attract organic acids (Weber and Van Vliet, 1980).

The effect of the adsorbate pH is important when the adsorbent is capable of ionizing in response to the prevailing pH. When the pH is such that an adsorbate compound exists in ionized form, adjacent molecules on the carbon surface will repel each other because they possess the same charge. Thus, adsorbate molecules cannot occupy adjacent adsorption sites and the equilibrium amount of adsorbed solute is low. In contrast, when the adsorbate is not ionized, no electrical repulsion exists and the adsorbate molecules can pack closely together on the surface of the carbon. In general, acidic species adsorb better at low pH, and basic species adsorb better at high pH (Cooney, 1999).

2.5 Applications of Activated Carbon

The use of porous carbon dates back to 2000 B.C. when the Egyptians used it as an adsorbent for medicinal and purification purposes (Patrick, 1995). The industrial use of activated carbon began in the early 1900's in the sugar refining process. Higher quality gas adsorbing GAC was used in gas masks to protect against poisonous gases during World War I. Today, GAC has diverse applications in the food, pharmaceutical, chemical, and petroleum industries as well as in the treatment of potable water and municipal and industrial wastewater. The most common impurities removed by AC include pesticides, aromatic hydrocarbons, detergents, phenols and their derivatives, and carcinogenic compounds. Nearly 80% (300,000 tons/year) of the total AC consumed in the world is used for liquid phase applications (Patrick, 1995).

14

PAC is mainly used for adsorption from solution since its fine particles have less diffusional resistance. In water treatment, PAC is used in conjunction with the coagulation process. Because PAC is difficult to separate from the liquid effluent, it is rarely regenerated.

GAC is commonly used for the adsorption of gases since it permits the passage of a carrier gas through a bed of carbon without an excessive pressure drop. GAC is also extensively used for the adsorption of liquids. In liquid applications, GAC is more desirable for continuous or cyclic processing using fixed-beds since pressure drop can be controlled by adjusting the particle-size distribution. Although GAC is more expensive than PAC, it tends to be more cost-effective for high usage rates because it can be regenerated.

2.6 Liquid-Phase Adsorption Systems

The three commonly used continuous flow liquid-phase adsorption systems for GAC are fixed-bed, pulsed-bed, and fluidized-bed. These systems can be operated singly, in series, or in parallel. The typical activated carbon contact system consists of a cylindrical tank with a bed depth of 3-10 meters of GAC (U.S. EPA, 1973). Contaminated influent is passed either up (upflow) or down (downflow) through the bed with sufficient residence time for the completion of the adsorption process. The flow rate necessary for optimum performance depends upon the rate of adsorption by GAC. In general, flow rates range from 0.5-2.6 lpm/m^2 of cross-sectional area (U.S. EPA, 1973).

2.6.1 Fixed-Bed

As shown in Figure 2.2, in a fixed-bed adsorber, contaminated influent is introduced from the top of the adsorber over a fresh bed of GAC. The upper zone of the carbon begins to remove adsorbate until it becomes saturated at a level corresponding to the influent concentration (C_0). Successive layers of carbon

15
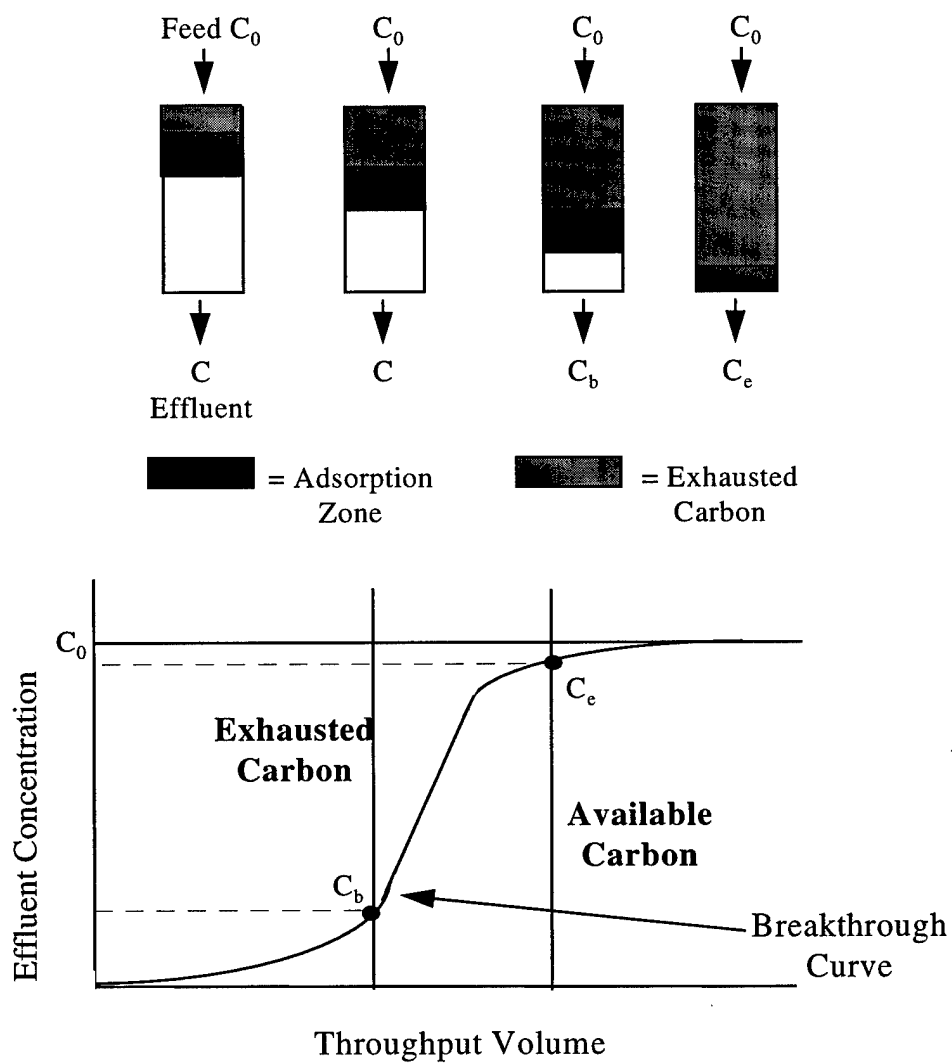
Figure 2.2 Adsorption Zone Progression in Fixed-bed Adsorber (Droste, 1997).

16

have lower accumulations of adsorbate since they are subjected to lower concentrations of adsorbate in the liquid. At a certain point, the adsorbate concentration in the liquid will decrease to nearly zero and the carbon below this point will be adsorbate free. By definition, this area where concentration decreases from the influent value to essentially zero is the adsorption or mass transfer zone (Droste, 1997). As the top layers of carbon become saturated, the adsorption zone moves downward until the entire bed becomes exhausted. When the leading edge of the adsorption zone reaches the bottom of the column, a detectable amount of adsorbate begins to appear in the effluent. At a predetermined time or breakthrough concentration (C_b), flow to the adsorber is stopped and the carbon bed is replaced.

The relationship between the volume of liquid passing through the carbon column and concentration in the effluent is used to plot a breakthrough curve. The area above the curve represents exhausted carbon while the area below the curve represents essentially virgin carbon. The exhaustion concentration (C_e) varies with the shape of the breakthrough curve. For a gradually sloped curve, the value is near 0.90 C_0 and for a steeply sloped curve the value is near 0.99 C_0 (Droste, 1997). The flow rate of adsorbate through the column affects the shape of the curve. As the flow rate increases, the slope of the curve decreases and breakthrough begins earlier since the depth of the adsorption zone increases as there is less time for adsorption in each layer (Chakravorti and Weber, 1975).

The advantage of a downflow fixed-bed is that the filtration of suspended solids and adsorption occur simultaneously. However, periodic backwashing is necessary to limit headloss due to clogging. A disadvantage of a fixed-bed system is the large fluctuation in the concentration of effluent as breakthrough is reached. To limit the effect of breakthrough from a single column, the system in normally operated using multiple columns in parallel.

2.6.2 Pulsed-Bed

In a pulsed-bed, liquid enters through the bottom of the adsorber and leaves through the top. At periodic intervals, the flow of liquid is stopped and exhausted carbon is removed from the bottom. The typical system in operated so that no more that 10% of the carbon is pulsed at any one time. Virgin or regenerated carbon is added to the top of the adsorber.

A pulsed-bed incorporates a countercurrent operation where flow of the influent and solid adsorbent are in opposite directions. The highest concentrations of adsorbate contact the most nearly exhausted carbon while the fresh carbon contacts the lowest concentrations of adsorbate. This system takes full advantage of the adsorption capacity of the nearly exhausted adsorbent.

2.6.3 Fluidized-Bed

One of the problems associated with carbon adsorbers is plugging of the bed by suspended solids in the influent. An alternative is to use a carbon bed in a fluidized state. Sufficient upflow is provided to maintain the bed at about 10% expansion to allow the suspended solids to pass through. An advantage of a fluidized-bed is significant improvement in mass transfer and mixing due to turbulent flow. Additionally, adsorbed organic molecules increase the density of the carbon and the exhausted carbon migrates to the bottom of the bed for easy removal.

2.7 Regeneration of GAC

The objective of the regeneration of GAC is to desorb accumulated adsorbates and restore the original porous structure with little or no damage to the carbon itself. GAC can be regenerated by a variety of methods, but the process fundamentals are essentially the same. In most processes, regeneration is accomplished by subjecting the exhausted carbon to conditions that shift the

18

adsorption equilibrium in favor of desorption. The relative ease of regeneration is dependent upon the type of adsorption (physical or chemical).

For physiosorption, this shift can usually be accomplished by heating, lowering the pressure, or washing with solvent. In the case of chemisorption, a supply of energy greater than the sorptive force is required to break the strong ionic or covalent bonds.

The most common method used for the regeneration of GAC is the thermal process. In addition to thermal regeneration, other methods discussed in the following sections include wet air oxidation, chemical, and solvent regeneration. No matter which method is used, it is important to note that the regeneration of GAC is dependent upon the characteristics of the base material, the activation process, and the type or types of adsorbate.

2.7.1 Thermal Regeneration

Thermal regeneration of GAC involves three steps: drying, baking (pyrolysis of adsorbates), and reactivation (oxidation of the residue from the adsorbate). The process is conducted using multiple-hearth furnaces, rotary kilns, or fluidized-bed furnaces (Cheremisinoff and Morresi, 1978). In most cases, regeneration is conducted on-site. Some small-scale operations ship the spent carbon back to the manufacturer for regeneration.

A typical on-site regeneration system is shown in Figure 2.3. A wet slurry of spent carbon is hydraulically pumped to a dewatering bin where it drains by gravity. After reaching a moisture content of 50%, the exhausted carbon enters the furnace (McGinnis, 1984).

As the temperature is raised to 200 °C, the GAC dries and volatile adsorbates are released as gases. As the temperature of the carbon is raised to 400-600 °C, reversibly adsorbed substances are driven off while irreversibly adsorbed substances decompose and leave behind a char residue. During reactivation, the

19
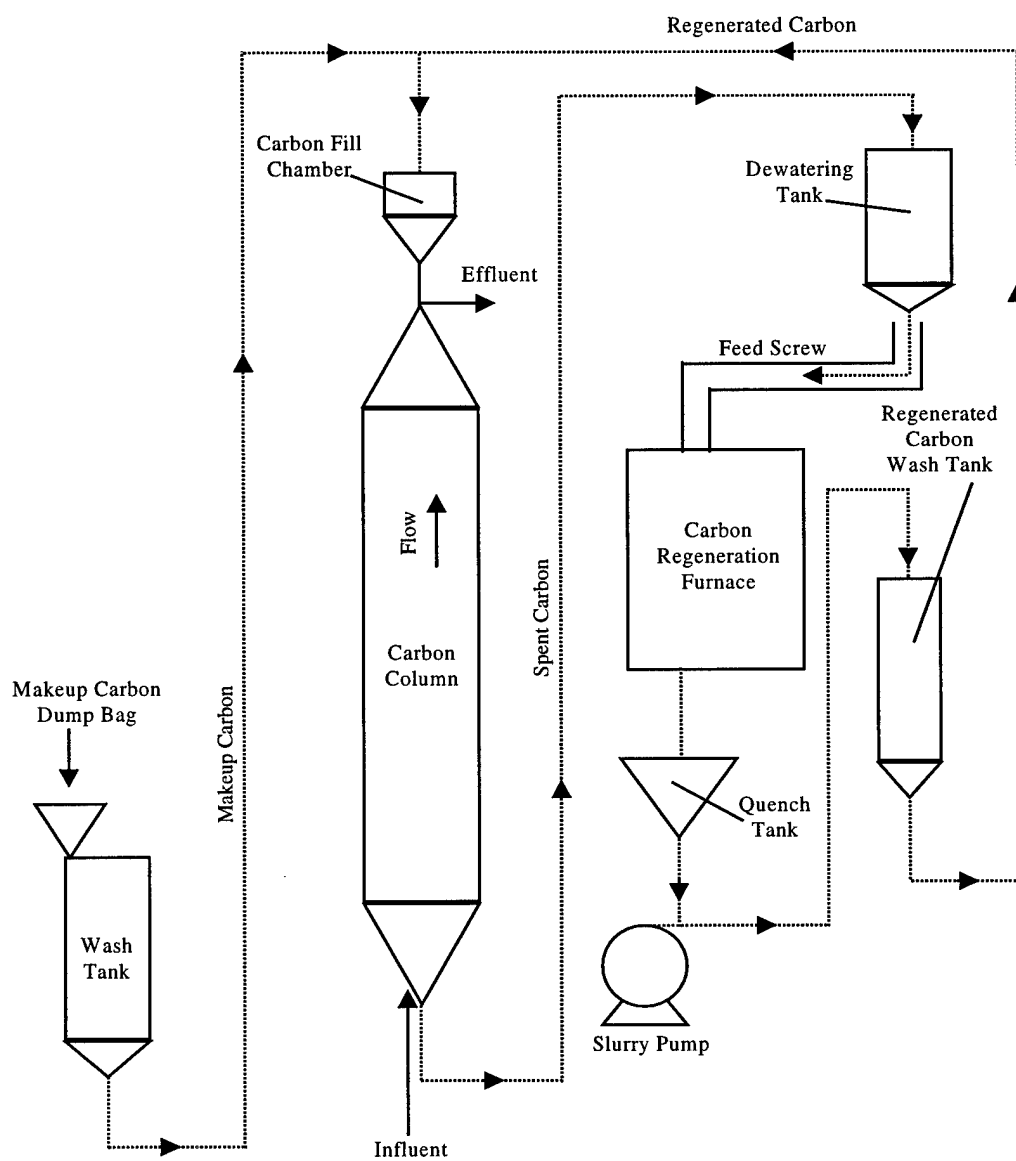
Figure 2.3 On-site Carbon Treatment and Regeneration System (Droste, 1997).

carbon is heated to 870-1000 °C in an atmosphere containing a high concentration of steam or CO_2 that oxidizes the char residue (Zanitisch and Stenzel, 1978). The detention time and amount of oxidant required is dependent on the particular adsorbate or adsorbates.

The hot regenerated carbon is discharged from the furnace to a quench tank where it is cooled and washed in water to remove fine particles before being pumped back to the adsorption vessel or storage tank. The entire process is complete in about 30 minutes (15-minute drying , 5-minute baking, and a 10-minute oxidation).

An advantage of thermal regeneration is that it can be used for carbons loaded with a heterogeneous mixture of adsorbates. Van Vliet (1991) characterized the responses of different compounds to thermal regeneration. Type I compounds are volatile organic compounds that are not irreversibly bound and easily undergo thermal desorption. Type II compounds are more tightly bound to activated carbon and do not undergo thermal desorption. Instead, they undergo thermal decomposition or cracking and form volatile fragments. Type III compounds are those which undergo pyrolysis and leave behind a carbonaceous residue. Both Type II and Type III compounds need a controlled oxidation step to remove the carbonized residue.

The reactions that occur during reactivation are identical to those in the activation step of AC production. Combustion conditions within the furnace are controlled to limit oxygen content to effect oxidation of the adsorbate rather than the carbon (Van Vliet, 1991).

Steam and CO_2 are commonly used reactivating gases and involve the following reactions (Patrick, 1995):

$$C + H_2O \rightarrow CO + H_2 \qquad (\Delta H = + 130 \text{ kJ mol}^{-1})$$

and

$$C + CO_2 \rightarrow 2CO \qquad (\Delta H = +159 \text{ kJ mol}^{-1})$$

Since both reactions are endothermic they can theoretically be controlled to oxidize the pyrolyzed adsorbate without damaging the surface of the carbon. However, since it is difficult to control process conditions at such high temperatures, there is invariably some oxidation of the carbon surface. For reactivation at temperatures of 950 °C, even short residence times can lead to excessive oxidation of selected carbons (Van Vliet, 1991). In most cases, there is a 5-10% loss of carbon due to surface oxidation.

A field method used to estimate regeneration efficiency is apparent density (weight per unit volume). As GAC is regenerated, organic molecules are removed and the carbon loses weight. If the apparent density of the regenerated carbon is greater than that of virgin carbon, the carbon is retaining some of the adsorbed material. If the apparent density of regenerated carbon is less than virgin carbon, the carbon is being oxidized in the furnace (Smithson, 1978).

One disadvantage of thermal regeneration is a loss of adsorption capacity caused by changes in the pore structure of the carbon. Van Vliet (1991) studied pore volume changes associated with reactivation of non-contaminated virgin GAC over a 60-minute residence time at 950 °C. It was reported that during the first ten minutes there were small increases in the volumes of micropores and macropores due to further activation. However, during the next 50 minutes there was a 44% loss of micropore volume and increases in the mesopore and macropore volumes of 66% and 50%, respectively. These physical changes were attributed to the burning out of the walls between micropores. As a result, the surface area available for the adsorption of smaller molecules was significantly reduced which resulted in a decrease of adsorption capacity. When larger molecules were adsorbed, the loss of micropore volume had a minimal effect on adsorption capacity.

22

Other disadvantages associated with some forms of thermal regeneration include high energy requirements, air pollution problems associated with off gasses, and incompatibility of some adsorbates with high temperature operations. For example, thermal regeneration can not be used with explosive adsorbates such as TNT (Lyman, 1978).

Magne and Walker (1986) and Ferro et al. (1993) reported that thermal regeneration of GAC previously contaminated with phenol did not restore total adsorption capacity. These studies showed that phenol adsorbed by both physiosorption and chemisorption. During regeneration, the physically adsorbed portion of phenol desorbed thermally; however, the chemically adsorbed portion was pyrolyzed by the high temperatures before it was desorbed. As a result, the total surface area as well as the surface area accessible to phenol decreased (Ferro et al., 1993).

2.7.2 Wet Air Oxidation

Wet air oxidation (WAO) is an aqueous phase oxidation process that uses molecular oxygen as an oxidant. The process operates at temperatures from 125 °C to 320 °C and pressures from and 0.5-20.3 MPa (Knopp et al., 1978). Oxidation conditions vary, depending on whether partial or complete oxidation is desired.

Mundale et al. (1991) studied the regeneration of activated carbon loaded with phenol. Using a WAO process, experiments were conducted at temperatures of 150 °C and 185 °C and an oxygen partial pressure of 0.5 MPa. They reported 5-10% and negligible losses, respectively, at temperatures of 185 °C and 150 °C. The loss of adsorption capacity was attributed to surface oxidation as well as the formation of carbon-oxygen complexes on the surface of the carbon.

The rate controlling step was found to be the reaction between the dissolved oxygen and the desorbed phenol. A second set of experiments conducted using

23

non-contaminated carbon showed that surface oxidation occurred even in the absence of the adsorbate.

A study by Gitchel et al. (1980) reported that an increase in activation was observed after wet oxidation of non-contaminated GAC. For temperatures ranging from 200-300 °C, a pore volume greater than virgin GAC was observed for all pore diameters. The largest increase in volume was observed in pore diameters greater than 600 angstroms.

2.7.3 Chemical Regeneration

Chemical regeneration is a process in which adsorbates are removed from spent carbon by reacting with suitable chemical reagents. In general, two types of reagents are used: those with oxidizing ability and those with solubilizing ability. Subsequent washing with water is required to remove the regenerating agent.

Chemical regeneration exhibits several advantages over thermal regeneration. The process can be done in situ which eliminates losses due to pumping, transport, and repacking. Additionally, carbon loss due to burn-off is eliminated and the recovery of adsorbates is possible by using subsequent treatment methods such as distillation.

The disadvantages associated with chemical regeneration include the high cost of reagents, danger of pollution from hazardous chemicals, and incomplete regeneration. The amount of regeneration is dependent primarily on the solubility of the adsorbate in the regenerant solution. Additionally, since most industrial wastewater contains a heterogeneous mixture of adsorbates, multiple regenerants are required.

Literature shows mixed results for the chemical regeneration of GAC exhausted with phenol. Leng and Pinto (1996) reported that the solubility of organic adsorbates and surface characteristics of the adsorbent strongly influence regeneration efficiency. By using reactive reagents and controlling surface charge

characteristics through pH, they were able to enhance the solubility of selected organic adsorbates in aqueous solutions. For phenol, an adsorbate that is difficult to solubilize and is strongly bound to the surface, reduced affinity for the adsorbent caused by changes in surface charge was most effective. Himmelstein et al. (1973) reported that desorption of phenol with a 4% aqueous solution of sodium hydroxide was effective. It was postulated that the reaction produced water soluble sodium phenolate that was easily desorbed from the surface of carbon. Additionally, the high pH resulting from the sodium hydroxide modified the polarity of surface oxides and reduced the attraction between phenol and the GAC. In contrast, Magne and Walker (1986) reported that a portion of phenol becomes chemisorbed and can't be removed by chemical solvents.

2.7.4 Solvent Regeneration

Solvent regeneration is an extraction process that involves passing a solvent through a bed of exhausted carbon to dissolve the adsorbed material. Two types of extraction discussed in literature include subcritical water regeneration and supercritical CO_2 regeneration.

Salvador and Sanchez (1996) studied subcritical water regeneration (300 °C and 12.2 MPa) of three types of carbon exhausted with phenols, textile dyes, and pesticides. They reported that phenol desorbs at low temperature (155 ° C), dyes (sirrus red) at medium temperature (263 °C), and carbofuran, a pesticide, begins to release at 100 °C but does not completely desorb until above 325 °C. For all cases, even after seven regenerations, complete regeneration of the virgin adsorption capacity was achieved. In some cases, there was even an increase in adsorption capacity after the first regeneration. This increase was attributed to a slight increase in carbon activation caused by dissolved gases or a better cleaning of the pores with high temperature water.

Regeneration of spent activated carbon with supercritical CO_2 has been proposed as an alternative to conventional thermal regeneration (Modell et al., 1980). A significant advantage of supercritical CO_2 is its low critical temperature (31.06 °C) and critical pressure (7.38 MPa).

Studies investigating the use of supercritical CO_2 to regenerate GAC have shown mixed results. It appears the ease of regeneration is dependent upon the strength of adsorption. In most cases, the results indicated that a steady state adsorption capacity was achieved by supercritical CO_2 regeneration. For GAC exhausted with phenol, Modell et al (1980) reported a 20% decline in adsorption capacity after one regeneration stage. This 20% reduction remained constant during successive cycles and was attributed to irreversible binding of phenol to surface oxides during the first adsorption cycle. The surface oxides provided high-energy sites capable of chemisorption. In the same study, they reported complete restoration of activated carbon exhausted with acetic acid after each of eight adsorption and regeneration cycles.

Tan and Liou (1988) and Srinivasan et al. (1990) investigated the desorption of ethyl acetate, an adsorbate not as strongly adsorbed as phenol, in a packed-bed column using supercritical CO_2. Both studies reported a loss of adsorption capacity during the first three regeneration cycles; however, after the third regeneration cycle there were no further losses. Overall, 87% of the original adsorption capacity was restored. De Filippi et al. (1980) studied the regeneration of carbon exhausted by pesticides with supercritical CO_2. This study showed that the high solubility of certain pesticides in supercritical CO_2 did not insure that they could be removed from the GAC.

Kinetic studies by Recasens et al. (1989) and Tan and Liou (1988) reported that desorption with supercritical CO_2 was influenced by flow rate and pressure. Increased flow rates of the supercritical CO_2 resulted in decreased desorption time while higher pressures were more favorable for regeneration.

26

2.8 Properties of Supercritical Water

As illustrated in Figure 2.4, water becomes a supercritical fluid above a temperature of 374 °C and a pressure of 22.1 MPa (McHugh and Krukonis, 1994). As the temperature and pressure of a liquid and gas in equilibrium increase, thermal expansion causes the water to become less dense. At the same time, the gas becomes denser as the pressure rises. At or above the critical point, the densities of the two phases become identical and the water exists as a single-phase fluid.
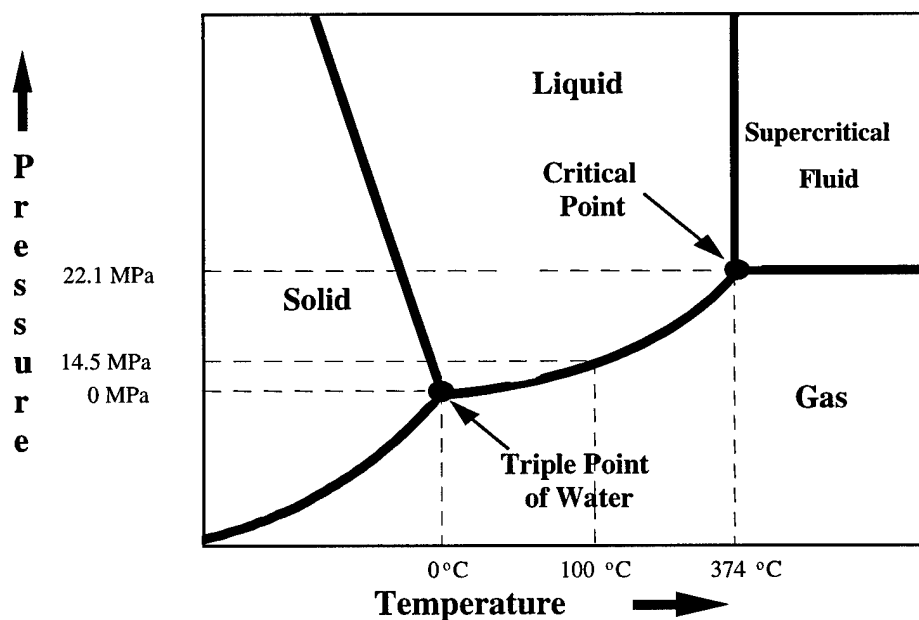
Figure 2.4 Phase Diagram for Water.

In the supercritical region, the physical-chemical properties of water are significantly different than either liquid or vapor water. For example, density, viscosity, and dielectric constant are significantly altered.

27

The solvent strength of SCW is related to its density. By varying pressure and temperature, the density of SCW can be controlled between gas-like and liquid-like. Figure 2.5 shows the effect of temperature on the density of water at a constant pressure of 26.2 MPa. The density of water is 1.0 g cm^{-3} at 25 °C and gradually decreases to 0.5 g cm^{-3} at the critical point. Above the critical point, the density of water decreases rapidly and can drop to as low as 0.1 g cm^{-3} at 500 °C (Josephson, 1982). These changes in density are caused by an increase in the thermal energy of the water molecules. As the water molecules move further apart, the affect of hydrogen bonding is reduced and the concentration of polar molecules decreases.
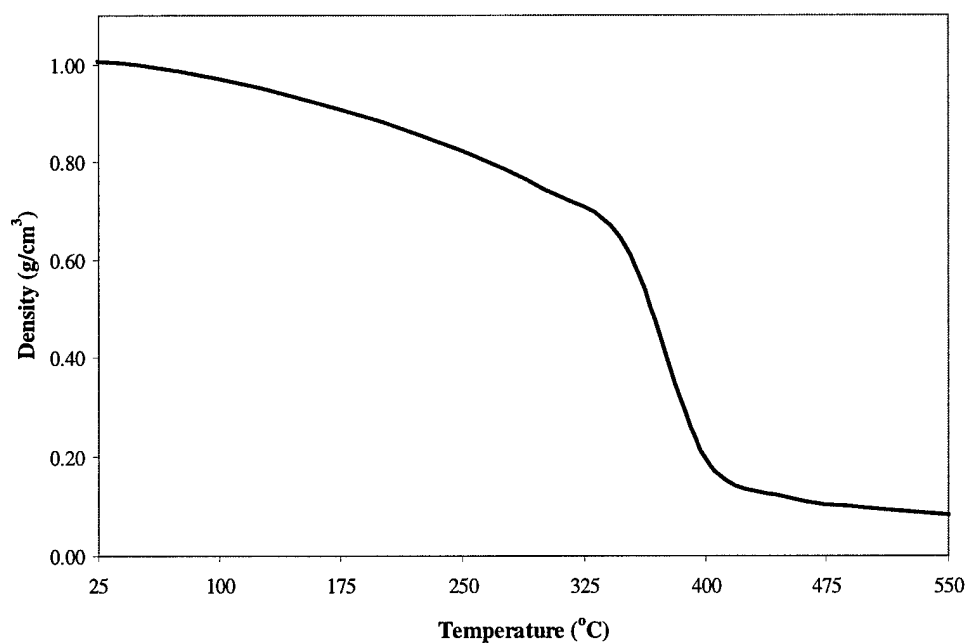
Figure 2.5 Temperature Dependence on the Density of Water at 26.2 MPa.

The low density and reduced hydrogen bonding is also associated with a decrease viscosity as shown in Figure 2.6. Compared to liquid solvents, SCW exhibits high diffusivity and low viscosity that facilitates rapid extraction and phase separation.
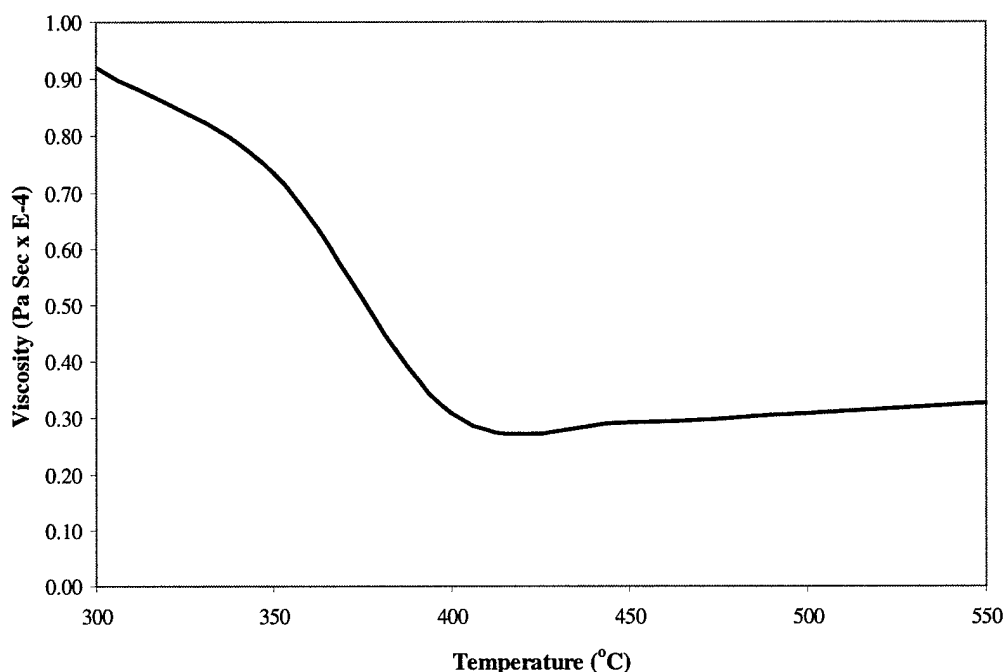
Figure 2.6 Temperature Dependence on the Viscosity of Water at 26.2 MPa.

The dielectric constant, which is a measure of polarity and hydrogen bonding, also decreases under supercritical conditions. The dielectric constant, as a function of temperature, changes at a greater rate than the density. At ambient conditions, the dielectric constant for water is 80, which makes ambient water a good solvent for many inorganic species. However, under supercritical conditions the dielectric constant can drop to as little as 2.5 (Josephson, 1982). Because of the low dielectric constant, SCW poorly shields the electrostatic potential between ions and dissolved ions exist largely as contact ion pairs (Shaw et al., 1991). As a

result, SCW exhibits characteristics of a non-polar organic solvent. Organic compounds that are only slightly in water at standard conditions are completely miscible in SCW. SCW is also miscible with gases such as oxygen, helium, hydrogen, nitrogen, and carbon dioxide. However, the same properties that make SCW an excellent solvent for non-polar organic compounds, such as benzene and toluene, make it a poor solvent for many inorganic compounds, such as salts and inorganic oxides.

3.0 EXPERIMENTAL METHODS AND PROCEDURES

Experiments were conducted using specially designed bench-scale adsorption and regeneration apparatuses. This chapter describes the experimental equipment, operational and analytical procedures, and chemicals used during this study. Schematics and descriptions of the adsorption and regeneration apparatuses are included.

3.1 Adsorption Apparatus

Figure 3.1 depicts a schematic of the adsorption apparatus. A high-pressure feed pump (Milton Roy, Model No. 396-31; later replaced by Water's M45 solvent delivery system) equipped with adjustable flow capability was used to pump the influent phenol solution from a 1000-mL separatory funnel through the vertically mounted packed-bed adsorption column. A 6.35 mm O.D. polyethylene tube was used to transport the feed from the pump to the adsorption column.

The packed-bed adsorption column was constructed from stainless steel 316L tubing (19 mm O.D. x 16 mm I.D. x 2.25 cm long). The internal volume of the column was 6.84 cm^3. Effluent samples were collected in a 100-mL graduated cylinder.

3.2 Adsorption Procedures

Virgin GAC was washed with distilled and deionized (DDI) water and dried in an oven at 105 °C for 24 hours. After drying, the GAC was removed from the oven and allowed to equilibrate. The equilibration step was necessary since dried carbon can gain as much as 5-10% in weight when exposed to ambient temperature and humidity (Randtke and Snoeyink, 1983). After reaching a constant weight, the GAC sample was loaded into the adsorption column. The adsorption stage was initiated by pumping phenol solution from the separatory funnel through the adsorption column at a constant flow rate. Effluent samples

**1000-mL
Separatory Funnel**

**Packed-Bed
Adsorption Column**

P

Pressure Gauge

**Graduated
Cylinder**

Feed Pump
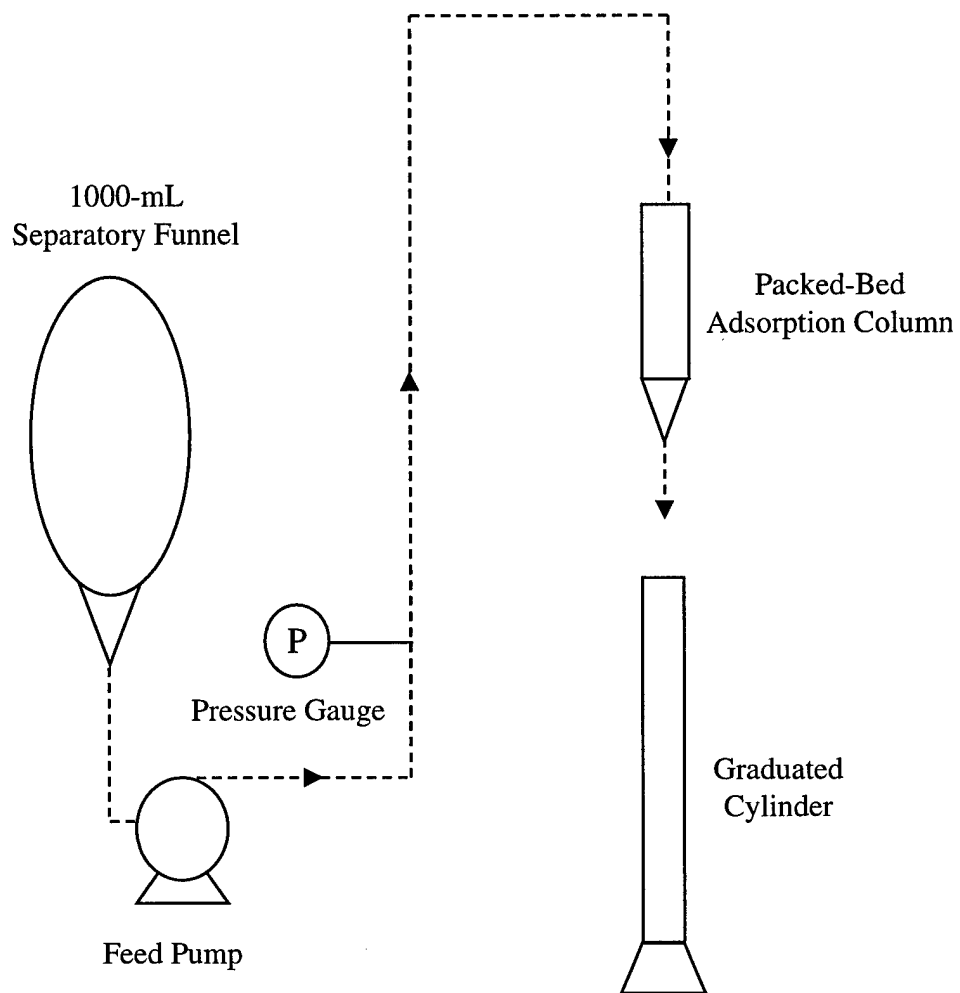
Figure 3.1 Fixed-bed Adsorption Apparatus.

were collected in 5 mL increments for first 30 mL and every 10 mL thereafter. The adsorption cycle was stopped after 120 mL of feed solution passed through the adsorption column. Each adsorption cycle lasted approximately one hour.

At the completion of the adsorption stage, the adsorption column was removed from the apparatus and dried at 105 °C for 24 hours. After equilibration with ambient conditions, the weight of the dried contaminated GAC was recorded. To prevent readsorption of moisture, the carbon was stored in a desiccator until the regeneration stage.

3.3 Regeneration Apparatus

Figure 3.2 depicts a schematic of the bench-scale regeneration apparatus. A high-pressure feed pump (Milton Roy, Model No. 396-31; later replaced by a Williams, Model P250V225) equipped with adjustable flow capability was used to pump distilled and deionized (DDI) water from a 100 mL burette. From the discharge of the pump to the inlet of the desorption column there was approximately 6.4 m of 6.35 mm I.D. stainless steel 316L tubing, of which approximately 5.79 m was coiled inside the heat source for increased heat transfer to the water. The heat source was a high-temperature oven (Thermolyne Sybron with Turnatrol II Type 13300 controller, Model No. FA17730-1) measuring 39.37 cm wide x 22.86 cm deep x 22.86 cm high. 3.175 mm O.D. tubing was used in the vicinity of the oven door to allow the oven door to open and close. The desorption column (19 mm O.D. x 16 mm I.D. x 2.25 cm long) was identical to the adsorption column. To ensure adequate mixing, the desorption column was mounted vertically and arranged as a fluidized-bed. Two thermocouples (Omega Type K) measured the inlet and outlet temperature of the reactor. Inlet and outlet temperatures were displayed on a digital display (Omega Model Number CN4400 and CN9000, respectively). Pressure was monitored by a pressure gauge (U.S. Gauge), which was capable of displaying pressure from 0 to 68.95 MPa in 1.38

33
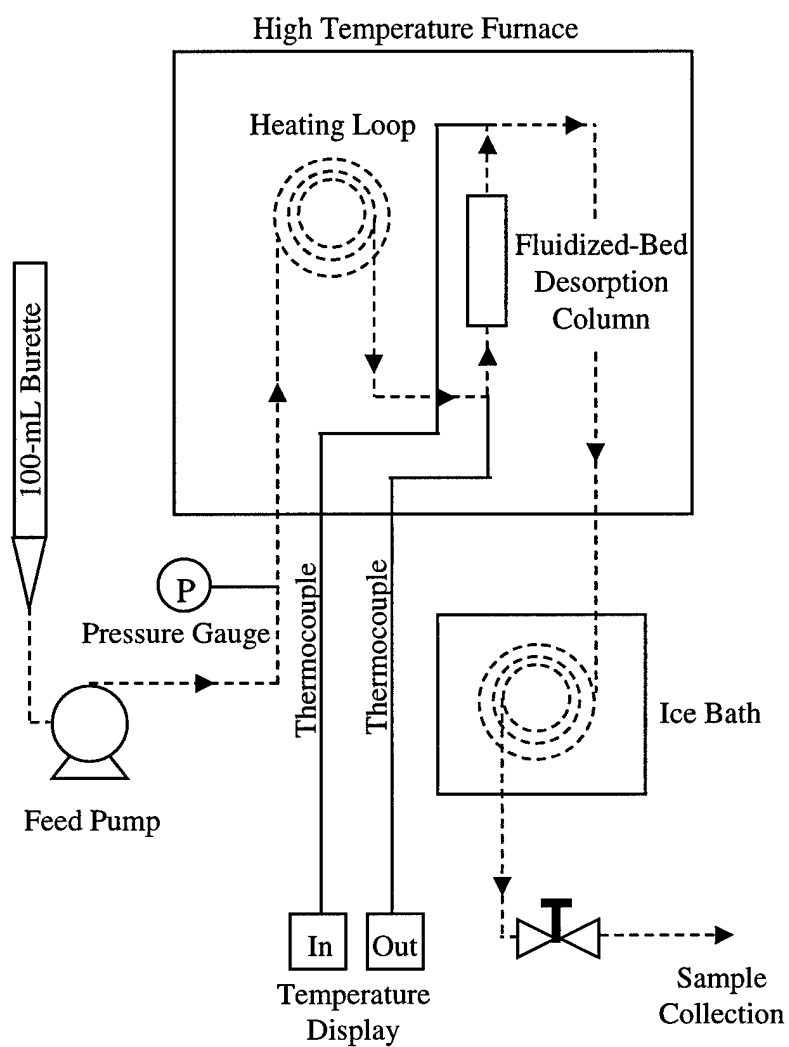
Figure 3.2 Bench-Scale Activated Carbon Regeneration Apparatus.

34

MPa increments.

In order to prevent washout of the GAC, a 2-micron in-line filter (Nupro Model No. SS-4TF) was placed at the outlet of the reactor and a 0.5 micron in-line filter (Nupro Model No. SS-SS-4TF) was located in the tubing ahead of the pressure let down valve seat. Pressure was controlled through a proportional pressure relief valve (Nupro, R3A Series, Model No. SS-4R3A), a metering valve (Whitney, 31 Series, Model No. SS-31RF2), and a micro-metering valve (Nupro, S Series, double-pattern, Model No. SS2-D) for fine control. Just prior to the pressure reduction valve, the effluent passed through an ice bath. This ice bath consisted of 80 cm long 3.175 mm O.D. coiled tubing immersed in a plastic beaker filled with ice water. Liquid effluent samples were collected from a four-way switch-valve using plastic 60-cc syringes.

3.4 Regeneration Procedures

Prior to a regeneration experiment, regenerant DDI water with the desired oxygen level was prepared. For experiments requiring no dissolved oxygen, DDI water was degassed for two hours by bubbling helium through a diffuser. Degassing continued during the entire regeneration stage. For experiments requiring 5 mg/L of dissolved oxygen, ambient DDI water was used. Dissolved oxygen levels for the degassed and DDI water solutions were measured using a dissolved oxygen probe. For experiments requiring 100 mg/L of dissolved oxygen, 0.6 mL of hydrogen peroxide (50% by weight) was added to 2000 mL of DDI water.

The first step of each regeneration stage was to load the dried GAC from the adsorption stage into the desorption column. The prepared regenerant water was then pumped through the system to pressurize it to the test conditions (26.2 MPa for supercritical experiments and 12.4 MPa for subcritical experiments). After reaching the test pressure, the pump was turned off and the regeneration apparatus

was placed in the high-temperature oven (pre-heated to 490 °C for supercritical experiments and 380 °C for subcritical experiments). During the heat-up phase, pressure was maintained at the test temperature. The pump was started when the reactor inlet temperature reached the test condition. The regenerant flow rate was 4.5 mL/min for all experiments. The regeneration system required from eight to ten minutes to reach experimental conditions. Inlet and outlet temperatures, pressure, and flow rate were recorded every minute during the first ten minutes and every 12 minutes thereafter for a period of five hours. Effluent samples were collected in 60 mL syringes and transferred to 20 mL vials. The time and quantity of liquid effluent collected for each sample was recorded. After collection, the vials were transferred to a refrigerator and stored at 4 °C prior to analysis.

At the completion of the regeneration stage, the high-pressure feed pump was turned off and the regeneration apparatus was removed from the furnace. After cooling to ambient conditions, the column was removed from the system and placed in an oven at 105 °C for drying. After drying for 24 hours, the weight of the regenerated carbon after equilibration was recorded. Between experiments the regenerated carbon was stored in a dessicator to prevent the readsorption of moisture.

3.5 Analytical Methods

The analytical procedures used in this study included total organic carbon (TOC), BET surface area, pore size distribution, and scanning electron microscopy. All liquid samples were stored in a refrigerator at 4 °C immediately after collection and were analyzed within 48 hours of collection. When not in used, the carbon samples were stored in a dessicator.

3.5.1 Total Organic Carbon (TOC) Analysis

Total organic carbon (TOC) analyses were conducted using a Shimadzu Analyzer (Model No. 5050). TOC analyses were performed on liquid feedstock (adsorption experiments) and effluent samples (both adsorption and regeneration experiments). The lower detection limit was 1 mg/L. TOC analyses were conducted according to Standard Method 5310C (Greenberg et al., 1992).

3.5.2 BET Surface Area and Pore Size Distribution

Virgin GAC and regenerated GAC samples were evaluated for surface area and pore size distribution using an ASAP 2010 Micromeritics Accelerated Surface Area and Porosimetry System. The ASAP 2010 automatically measured surface area and pore size based on the adsorption and desorption of nitrogen on the surface and in the pores of the GAC.

Prior to analysis, GAC samples were degassed for 15 hours under vacuum at ambient temperature to remove adsorbed gases. High purity helium was used to determine the free space within a sample. The adsorption phase was conducted with ultra pure nitrogen at 77.35 °K. Equation 3.1, commonly known as the "BET equation" was used to relate the total volume of nitrogen adsorbed to the equilibrium partial pressure (Micromeritics, 1995).

$$\frac{P}{v(P_S - P)} = \frac{1}{v_m c} + \frac{(c-1)P}{v_m c P_S} \qquad (3.1)$$

where: P = pressure

P_S = saturation vapor pressure

v = volume of nitrogen adsorbed at pressure P

v_m = volume of nitrogen monolayer

c = constant

At partial pressures less than 0.03 MPa the adsorption isotherm is linear as the initial monolayer is adsorbed. For each sample, the ASAP 2010 calculated the amount of nitrogen adsorbed at different pressures (P) and computed the values of $P/v(Ps-P)$. These values were then plotted versus the corresponding P/P_s values and the data set was regressed to a straight line using linear least-squares (Micromeritics, 1995). The y-intercept of the line was $1/v_mc$ and the slope of the line was $(c-1)/v_mc$. After calculating the volume of a monolayer of nitrogen (v_m) using the values of the slope and y-intercept, the BET surface area was calculated using 16.2 angstroms^2 as the area covered by a single nitrogen molecule (Micromeritics, 1995).

The algorithm used by the ASAP 2010 to calculate pore size distribution was based on the Barrett, Johner, and Halenda (BJH) method (Barrett et al., 1951). As part of the BJH method, the thickness of the adsorbate layer was calculated using the Halsey equation:

$$t = 3.54 \left(\frac{-5.0}{\ln\left(\dfrac{P}{P_0}\right)} \right)^{\frac{1}{3}}$$
(3.2)

where: t = thickness of adsorbed layer

P = pressure

P_S = saturation vapor pressure

3.5.3 Scanning Electron Microscopy

A JEOL JSM35C Scanning Electron Microscope was used to examine selected samples of virgin and regenerated GAC. Samples were mounted on aluminum disks using double-sided tape. Magnifications ranged from 100X to 10,000X.

38

3.6 Materials Used in the Study

The GAC used in this study was NORIT Row 0.8 Supra, a peat-based extruded carbon. The large total pore volume and pore size distribution of this carbon makes it well suited for removing contaminants associated with chlorine, ozone, and dissolved organic compounds (Jankowska et al., 1991).

The phenol used in this study was manufactured by the Aldrich Chemical Company (Lot # 16418TR). Phenol solutions were prepared using distilled and deionized (DDI) water. The DDI water was distilled by a Durastill distillation unit to remove inorganics and treated with an ion exchange bed to remove both cations and anions. Air (Wilson, ultra zero grade) was used to operate the TOC unit. Hydrogen peroxide (50% by weight) was used to produce the regenerant water containing the equivalent of 100 mg/L of oxygen. The hydrogen peroxide was manufactured by the Aldrich Chemical Company.

4.0 RESULTS AND DISCUSSION

A series of adsorption and regeneration experiments were conducted to investigate the ability of hydrothermal processes to regenerate GAC. Phenol contaminated GAC samples were regenerated using both supercritical and subcritical water that contained various amounts of dissolved oxygen. Comparative studies were conducted using non-contaminated GAC. The effects on regeneration efficiency, regeneration rate, BET surface area, pore volume, average pore diameter, and surface characteristics were evaluated.

4.1 Scope of Regeneration Experiments

The first set of experiments, designated A, B, C and D, were designed to study the regeneration of phenol contaminated GAC. In these experiments, GAC was subjected to four successive adsorption-regeneration stages. Each adsorption-regeneration stage was considered as one cycle. The adsorption conditions for each experiment were constant. Rapid adsorption breakthrough curves were achieved by using relatively small flow rates of concentrated phenol solution (9000 mg/L). In the first experiment, 240 mL of phenol solution was passed through three grams of GAC at a flow rate of 4 mL/min. However, the high phenol concentration destroyed several pump seals. In subsequent experiments, 120 mL of phenol solution was passed through 1.5 g of GAC at a flow rate of 2 mL/min. This change did not affect loading (g of phenol/g of carbon) due to the proportional reductions in the flow rate, throughput volume, and mass of carbon. Typical loading of virgin GAC was 0.24 to 0.25 g/g. A complete listing of adsorption data is located in Appendix A.

The second set of experiments, designated E, F and G, were designed to study the regeneration of non-contaminated GAC. In this case, non-contaminated GAC was subjected to five regeneration stages.

40

Regeneration time (five hours) and flow rate (4.5 mL/min) were constant for all regeneration stages. The total volume of water passed through the desorption column during each regeneration stage was approximately 1.35 L. Regeneration variables for each experiment are shown in Table 4.1.

Table 4.1 Regeneration Variables.

Experiment	A	B	C	D	E	F	G
Regeneration Temperature (^{o}C)	411	411	411	300	411	411	300
Regeneration Pressure (MPa)	26.2	26.2	26.2	12.4	26.2	26.2	12.4
Dissolved Oxygen (mg/L)	0	5	100*	5	0	100*	5

Note: * Equivalent of 100 mg/L by adding H_2O_2 as an oxidant.

1. Experiments A, B, C, and D involved phenol contaminated GAC.
2. Experiments E, F, and G involved non-contaminated GAC.

Temperature (411 °C) and pressure (26.2 MPa) for the SCW regeneration experiments were selected because water at these conditions is well within the supercritical region. At these conditions, the density and viscosity respectively, were 0.160842 g cm^{-3} and 0.29445E-04 Pa sec. The conditions used for the subcritical regeneration experiments (300 °C and 12.4 MPa) were the same as a previous study conducted by Salvador and Sanchez (1996). At these conditions, the density and viscosity respectively, were 0.720683 g cm^{-3} and 0.87438E-04 Pa sec.

4.2 Regeneration Efficiency

The overall economics of GAC recovery is dependent on its reuse during multiple adsorption-regeneration cycles. As a result, the objective of GAC regeneration is to desorb accumulated adsorbates and restore original adsorption capacity. The effectiveness of hydrothermal processes to regenerate GAC was

41

measured by regeneration efficiency. Regeneration efficiency (RE), which is the percentage of original adsorption capacity restored after regeneration, was calculated using the following equation:

$$RE, \text{ after } n \text{ cycles} = \frac{\text{adsorption capacity after } n \text{ regenerations}}{\text{adsorption capacity of virgin carbon}} \times 100$$

where:

$$\text{adsorption capacity (g phenol/g carbon)} = \frac{\text{total phenol adsorbed (g)}}{\text{initial weight of carbon (g)}}$$

The total phenol adsorbed onto GAC during each adsorption stage was determined by two methods. The first method was based on the difference in dry weight of the GAC before and after the adsorption of phenol. The second method used the following quantitative analysis:

total phenol adsorbed (g) =

(Influent TOC Concentration − Effluent TOC Concentration) x (mL of volume) x

$$\frac{1L}{1000mL} \times \frac{1g}{1000mg} \times \frac{95g \text{ phenol}}{72g \text{ carbon}}$$

The two methods for determining the total phenol adsorbed during each adsorption stage provided results that were in close agreement. The deviation between the two methods was approximately 10% by weight.

Regeneration efficiencies, after each of four adsorption-regeneration cycles, are shown in Figure 4.1. After one cycle with SCW, a RE of 100% or greater was

42

observed for all levels of dissolved oxygen tested (Experiments A, B, and C). The increase in adsorption capacity suggested an increase in the number of adsorption sites available to phenol after regeneration with SCW. Similar results, attributed to dissolved gasses in the SCW, were observed by Salvador et al. (1996).
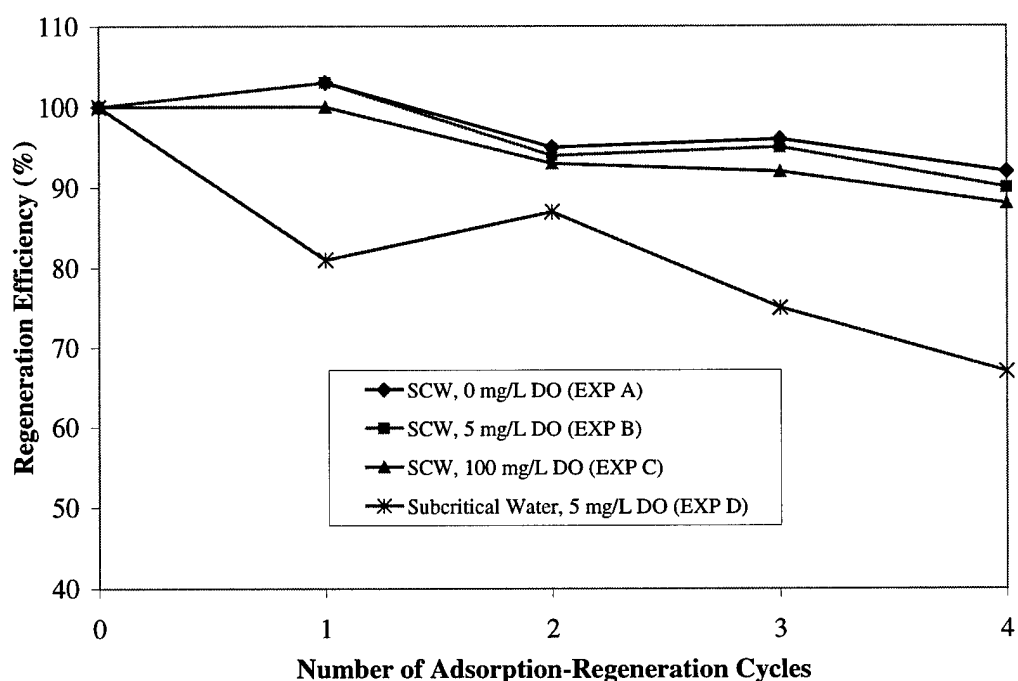
Figure 4.1 Regeneration Efficiency (%).

Although RE decreased during subsequent cycles, the overall adsorption capacity for GAC regenerated with SCW was well restored. RE after four cycles in SCW was 92%, 90%, and 88%, respectively, for dissolved oxygen concentrations of 0 mg/L, 5 mg/L, and 100 mg/L. Although a slightly higher RE was observed for degassed water, the differences were insignificant and indicated that dissolved oxygen concentration did not impact restoration of adsorption

43

capacity. However, the results using SCW did represent a significant improvement over the 20% loss of adsorption capacity reported by Modell et al. (1980) for the regeneration of phenol contaminated carbon using supercritical CO_2. It is postulated that the better results achieved with SCW, as opposed to supercritical CO_2 were related to temperature and molecular size. The higher temperatures associated with SCW resulted in increased thermal desorption and the smaller sized water molecules facilitated penetration into the smaller pores of the GAC.

The high RE observed for regeneration with SCW was not achieved for regeneration with subcritical water. Only 67% of the initial adsorption capacity was restored after four regeneration cycles with subcritical water (Experiment D). These results contradict the total recovery of adsorption capacity using subcritical water (300 $^{\circ}$C and 12.2 MPa) reported by Salvador and Sanchez (1996). It is postulated that the poor recovery of adsorption capacity observed in this study resulted from stoppage of the regeneration stage after five hours. If regeneration would have been conducted over a longer time, it is likely that a greater recovery of adsorption capacity would have been observed. However, the results did show that regeneration with SCW, as compared to subcritical water, was more rapid.

The better RE of SCW, as compared to subcritical water, was also evident by comparing the adsorption breakthrough curves in Figures 4.2 and 4.3. The area above each curve represents the adsorption capacity of the GAC. For regeneration with SCW (Figure 4.2), no decrease in adsorption capacity was observed after one cycle and only a 12% loss of adsorption capacity was observed after four cycles. In contrast, after regeneration with subcritical water (Figure 4.3), an 18% decrease in adsorption capacity was observed after one cycle and a 33% decrease was observed after four cycles.
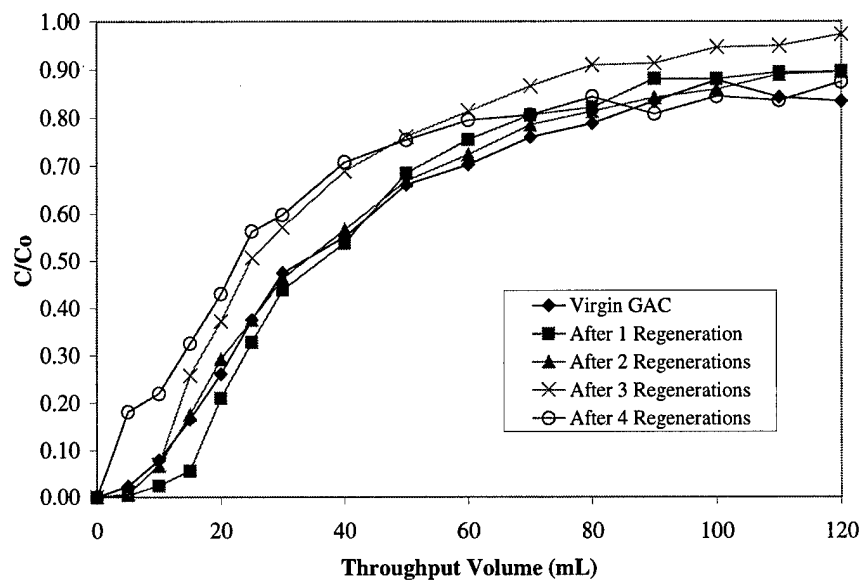
Figure 4.2 Breakthrough Curves after Regeneration with SCW (411 °C and 26.2 MPa) Containing 100 mg/L of Dissolved Oxygen (Experiment C).
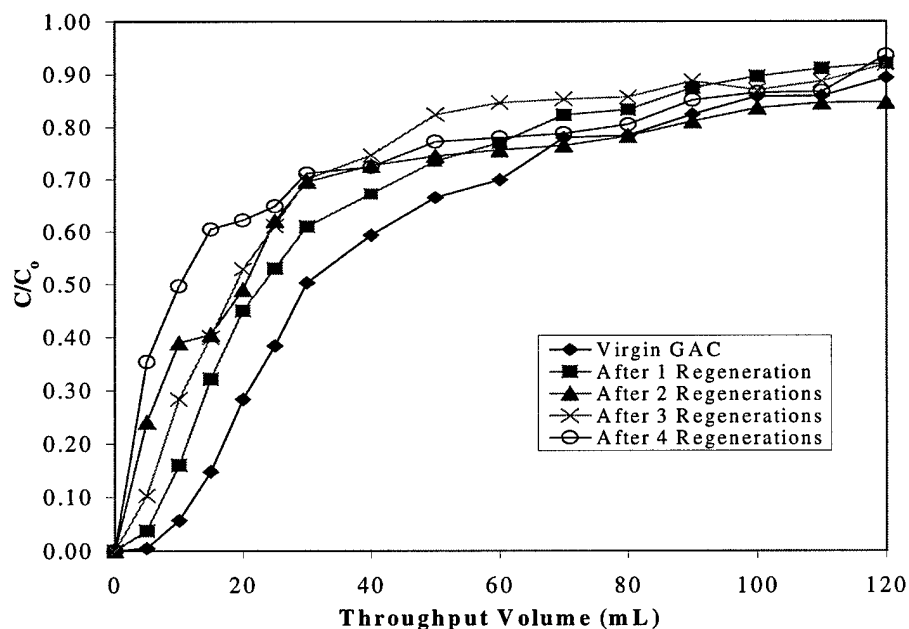
Figure 4.3 Breakthrough Curves after Regeneration with Subcritical Water (300 °C and 12.4 MPa) Containing 5 mg/L of Dissolved Oxygen (Experiment D).

45

4.3 Regeneration Rate

Phenol desorption rates for both subcritical and supercritical water are shown in Figure 4.4. These regeneration washout curves, observed during regeneration following the third adsorption stage, were typical of all regeneration stages in this study. A complete listing of regeneration data is located in Appendix B.
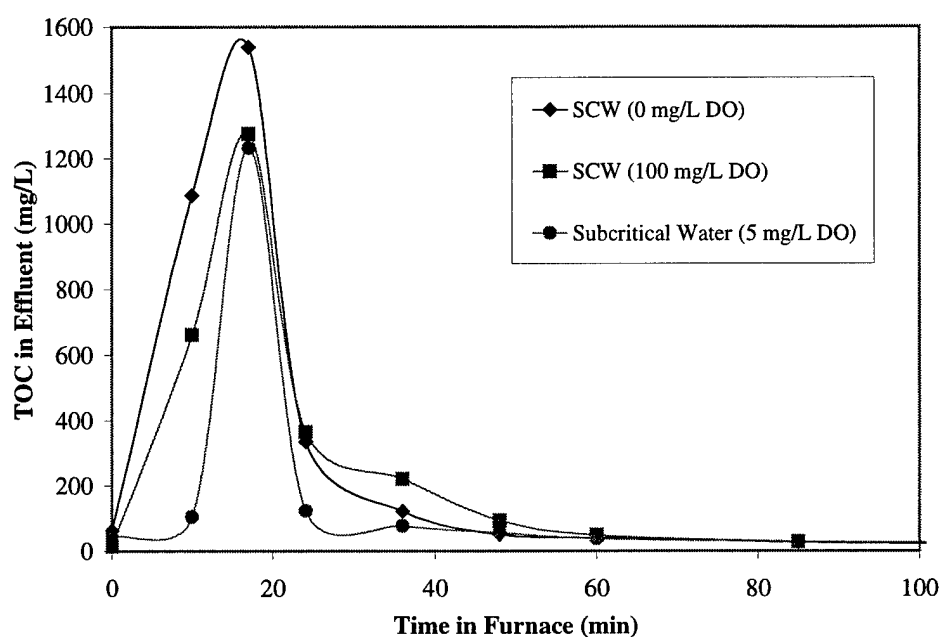
Figure 4.4 Regeneration Washout Curves after Three Adsorption-Regeneration Cycles.

The first ten minutes in the furnace were part of the heat-up phase in which temperature increased at a rate of 40 °C/minute. Pressure was kept constant at all times. The concentration of TOC in the effluent peaked soon after the onset of regeneration, decreased rapidly until 80-90% of the adsorbate was removed, and then decreased slowly until regeneration was complete. Overall, approximately 60% of the adsorbate was removed within 20 minutes and 90% within one hour. These results paralleled those reported by Modell et al. (1980) during regeneration

with supercritical CO_2.

The area under each curve represents the mass of adsorbate removed. The largest regeneration peak was observed during the degassed water trial (Experiment A) while the smallest peak was observed during regeneration with subcritical water (Experiment D). This trend corresponded to RE shown in Figure 4.1. Less adsorbate was removed during the subcritical water experiment; consequently, the regeneration efficiency of subcritical water was the lowest. It is likely that the higher diffusion rates and lower viscosity achieved in the use of SCW resulted in deeper and faster penetration into the GAC pores. Furthermore, the higher temperatures associated with SCW resulted in increased thermal desorption.

4.4 BET Surface Area

The extensive network of pores throughout a GAC particle provide the large surface area for adsorption to occur. The average surface area for two samples of virgin GAC, as determined by BET, was 928 m^2/g. The BET surface areas of phenol contaminated GAC after regeneration are shown in Table 4.2.

Table 4.2 BET Surface Area of Phenol Contaminated GAC after Regeneration.

Experiment	A	B	C	D
Regeneration Temperature (^{o}C)	411	411	411	300
Regeneration Pressure (MPa)	26.2	26.2	26.2	12.4
Dissolved Oxygen (mg/L)	0	5	100	5
Virgin Carbon (m^2/g)	928	928	928	928
After 2 Cycles (m^2/g)	706	692	609	569
After 4 Cycles (m^2/g)	522	533	528	371

A loss of BET surface area was observed after all cycles for all experiments. The greatest loss of surface area, nearly 60%, was observed after four cycles of regeneration with subcritical water (Experiment D). This corresponded to the lowest RE observed in Figure 4.1. In contrast, after four cycles of regeneration with SCW (Experiments A, B, C) there was an average 43% loss of surface area. For SCW, the effect of dissolved oxygen on loss of surface area was insignificant.

There were two likely reasons for the loss of surface area after regeneration of contaminated carbon. First, a portion of phenol was chemisorbed during adsorption, and it was not removed by either regeneration with supercritical or subcritical water. Second, there was pore plugging caused by decomposition products of phenol.

The losses of BET surface area observed after the regeneration of phenol contaminated carbon were not observed after regeneration of non-contaminated GAC. As shown in Table 4.3, the BET surface area of non-contaminated GAC after regeneration was greater than virgin GAC for all experiments.

Table 4.3 BET Surface Area of Non-contaminated GAC after Regeneration.

Experiment	E	F	G
Regeneration Temperature (^oC)	411	411	300
Regeneration Pressure (MPa)	26.2	26.2	12.4
Dissolved Oxygen (mg/L)	0	100	5
Virgin Carbon (m^2/g)	928	928	928
After 2 Cycles (m^2/g)	1036	1046	1034
After 4 Cycles (m^2/g)	1075	1034	1047

The overall increase in surface area after regeneration of non-contaminated GAC suggested that both supercritical and subcritical water exposures resulted in an increase in surface activation of the carbon. During regeneration, new pores developed and existing pores were either widened or deepened. The result was an increase in total BET surface area. The increase in surface area also indicated that excessive burn-off or surface oxidation did not occur during regeneration.

After four cycles, the greatest increase in surface area was observed for degassed SCW (Experiment E) and the smallest increase in surface area was observed for regeneration with the oxidant (Experiment F). Since all values were within 5%, the differences were insignificant and showed that the level of dissolved oxygen was not a significant factor in the change in surface area.

4.5 Pore Volume

Pore volume is the total volume of pores in a carbon particle per unit weight of the carbon (Cooney, 1999). In general, a carbon with a larger pore volume contains more adsorption sites and possesses a higher surface area than a carbon with a smaller pore volume. However, large pore volumes do not always correspond to high adsorption capacities. In terms of adsorption capacity, the distribution of volume between micropores (0-20 angstroms), mesopores (20-500 angstroms), and macropores (>500 angstroms) throughout the GAC is critical. Phenol, a relatively small molecule, is best adsorbed by GAC containing a large number of small adsorption sites.

Plots of cumulative pore volume versus pore diameter after two and four cycles are shown in Figures 4.5 and 4.6. In this case, GAC from Experiments A, C, and D were compared to virgin GAC. The cumulative pore volume represents the total volume contained in pore sizes of that diameter or less. The steepest part of the curve represents the pore diameter range where most of the pore volume is associated.

49
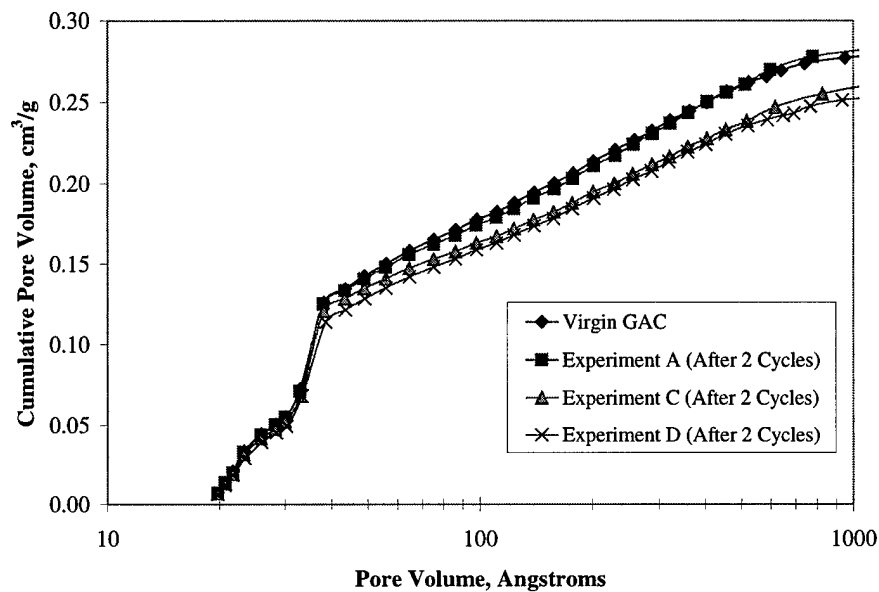
Figure 4.5 Cumulative Pore Volume Distribution (cm³/g) of Phenol Contaminated GAC after Two Adsorption-Regeneration Cycles.
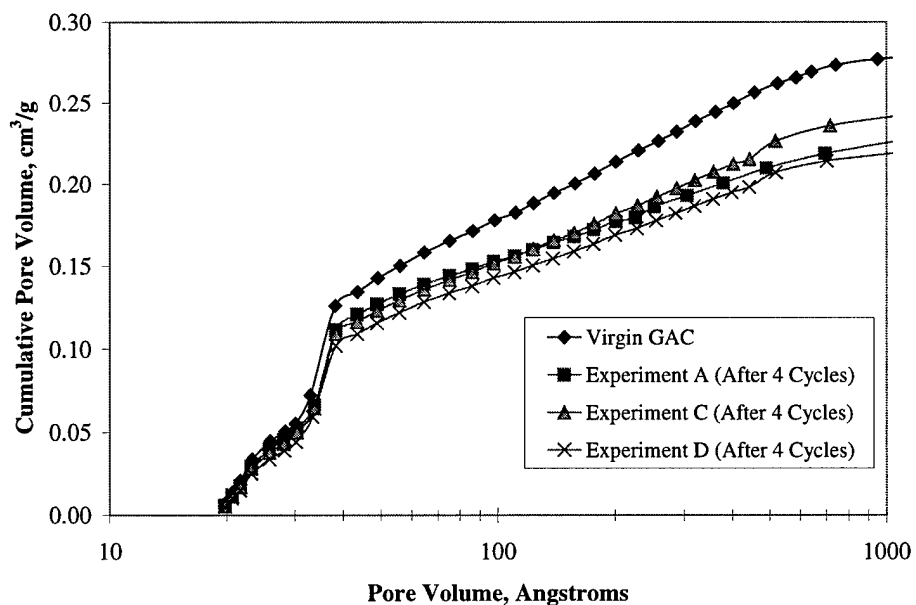
Figure 4.6 Cumulative Pore Volume Distribution (cm³/g) of Phenol Contaminated GAC after Four Adsorption-Regeneration Cycles.

From these plots, two trends were evident. First, there was a decrease in total pore volume across the entire range of pore diameters. Second, the largest cumulative volume was contained in pores with diameters between 30-40 angstroms.

As expected, the decrease in total pore volume paralleled the loss of surface area exhibited in Table 4.2. After four cycles (Figure 4.6), the largest loss of total pore volume was observed for regeneration with subcritical water (Experiment D), which corresponded to the largest decrease in surface area. The smallest loss of total pore volume was observed for regeneration with oxygenated water (Experiment C), which corresponded to the smallest decrease in surface area.

Cumulative pore distribution plots are useful for determining which size molecules are likely adsorbed by a particular GAC. However, conclusions based on total pore volume could be misleading since total pore volume reflects the net effect of changes in each pore region. The percent changes, after four cycles, in micropore, mesopore, and macropore volumes are shown in Table 4.4.

Table 4.4 Percent Change (from Virgin GAC) in Pore Volume after Four Adsorption-Regeneration Cycles.

Experiment	A	B	C	D
Regeneration Temperature (°C)	411	411	411	300
Regeneration Pressure (MPa)	26.2	26.2	26.2	12.4
Dissolved Oxygen (mg/L)	0	5	100	5
Micropore Volume (%)	-9	-11	-14	-25
Mesopore Volume (%)	-22	-23	-15	-22
Macropore Volume (%)	+18	+14	+23	+1

Losses of micropore and mesopore volume, accompanied by increases in macropore volume, were observed for all experiments. These changes were independent of dissolved oxygen concentration.

Assuming oxidation is a surface phenomenon that affects the larger pores near the outside of the carbon particle, the loss of micropore volume was caused by chemisorbed phenol and/or plugging of pores with decomposition products of phenol. The smallest losses of micropore volume, ranging from 9-14%, were observed after regeneration with SCW (Experiments A, B, C). In contrast, a 25% decrease in micropore volume was observed after regeneration with subcritical water. The lower surface tension and density of SCW likely allowed deeper penetration into the pores of contaminated GAC and resulted in a more efficient extraction process. Another possibility is that the oxidation of residual adsorbate is higher in SCW.

The percent losses of the micropore volume, 9%, 11%, 14%, and 25%, respectively for experiments A, B, C and D, mirrored the percent losses of adsorption capacity observed in Figure 4.1. This can be attributed to the fact that phenol is a relatively small molecule whose adsorption capacity was dictated by the volume of micropores and smaller-sized mesopores. Although volume changes in the larger pore regions affected surface area, they had little affect on the ability of the GAC to adsorb phenol.

The changes in mesopore and macropore volume provided evidence that some surface oxidation occurred during regeneration. The walls between mesopores eroded which created more macropores. Thus, there was a decrease in mesopore volume and an increase in macropore volume. The smallest increase in macropore volume, 1%, was observed after regeneration with subcritical water (Experiment D) which suggested that less surface oxidation occurred than with SCW. The amount of oxidation was independent of dissolved oxygen concentration.

Cumulative pore distribution plots for non-contaminated GAC after two and four regeneration cycles are shown in Figures 4.7 and 4.8. As with contaminated GAC, the largest cumulative pore volume was contained in the pores with diameters less than 40 angstroms. However, unlike the contaminated GAC, there was an increase in total pore volume after regeneration of non-contaminated GAC.

The percent changes in pore volumes for each pore region are shown in Table 4.5. For non-contaminated GAC, there was an increase across all pore volumes for all experiments.

Table 4.5 Percent Change (from Virgin GAC) in Pore Volume of Non-Contaminated GAC after Four Adsorption-Regeneration Cycles.

Experiment	E	F	G
Regeneration Temperature (^{o}C)	411	411	300
Regeneration Pressure (MPa)	26.2	26.2	12.4
Dissolved Oxygen (mg/L)	0	100	5
Micropore Volume (%)	+31	+23	+31
Mesopore Volume (%)	+12	+9	+5
Macropore Volume (%)	+28	+33	+16

The 23-31% increase in micropore volume supported the hypothesis that the loss of micropore volume observed after regeneration of phenol contaminated GAC was caused by chemisorbed phenol and/or pore plugging as opposed to oxidation of the carbon surface. In fact, the increases in micropore and mesopore volume observed in Table 4.5 provided further evidence that both subcritical and supercritical water caused an increase in the activation of the carbon. These results represent a benefit not observed during the thermal regeneration of non-
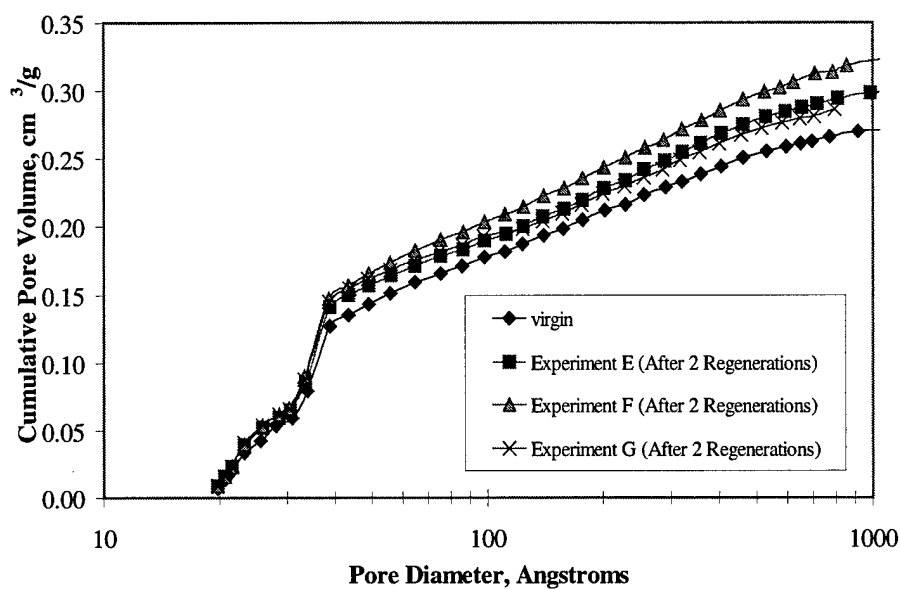
Figure 4.7 Cumulative Pore Volume Distribution (cm³/g) of Non-contaminated GAC after Two Adsorption-Regeneration Cycles.
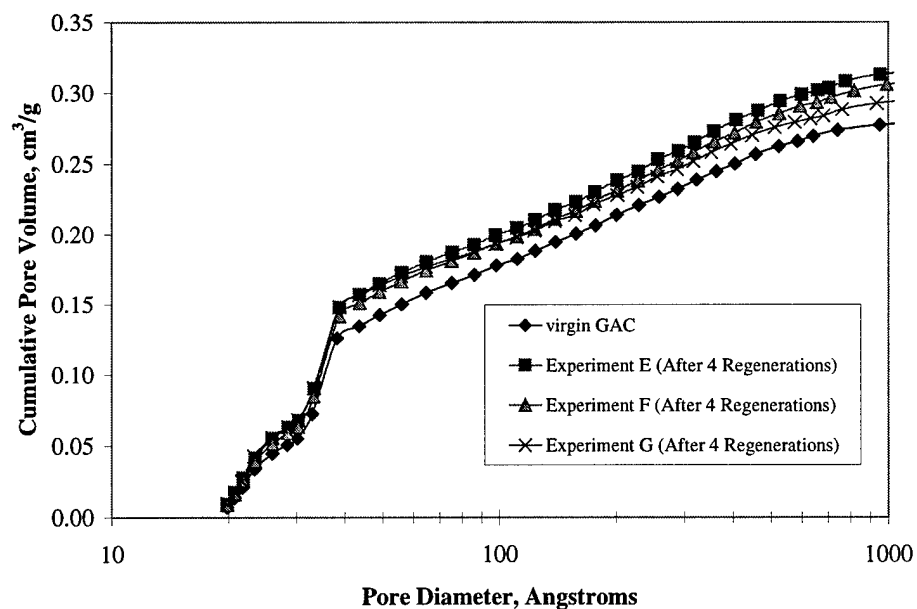
Figure 4.8 Cumulative Pore Volume Distribution (cm³/g) of Non-contaminated GAC after Four Adsorption-Regeneration Cycles.

54

contaminated GAC. For thermal regeneration, conducted at a temperature of 960 °C and a residence time of 60 minutes, Van Vliet (1980) reported an excessive loss of micropore volume and an increase in mesopore and macropore volume.

Meanwhile, the increases in macropore volume provided further evidence that oxidation did occur in the larger sized pores located near the surface of the GAC. The largest increases in macropore volume, 28-33%, were observed after regeneration with SCW. The smallest increase in macropore volume, 16%, was observed after regeneration with subcritical water. This suggested that surface oxidation was slightly greater under supercritical conditions. This was likely due to the higher temperatures involved.

4.6 Average Pore Diameter

Average pore diameters (4V/A), based on BET surface area and single-point total-pore volume, were calculated by an ASAP 2010 Micromeritics Accelerated Surface Area and Porosimetry System. These values were used to compare changes that occurred in overall pore size after contaminated and non-contaminated GAC samples were subjected to regeneration conditions.

The average pore diameters of phenol contaminated GAC after regeneration were compared to virgin GAC in Table 4.6. After two regeneration cycles with SCW, the average pore size increased approximately 14%. In contrast, a 21% increase in average pore size was observed after regeneration with subcritical water. These results further emphasized the advantage of supercritical water over subcritical water. A larger average pore size after regeneration with subcritical water was the result of less phenol removed from the micropores of the GAC and corresponded to the smallest RE, BET surface area, and total pore volume.

Table 4.6 Average Pore Diameter of Phenol Contaminated GAC after Regeneration.

Experiment	A	B	C	D
Regeneration Temperature (°C)	*411*	*411*	*411*	*300*
Regeneration Pressure (MPa)	*26.2*	*26.2*	*26.2*	*12.4*
Dissolved Oxygen (mg/L)	*0*	*5*	*100*	*5*
Virgin GAC (angstroms)	**23.88**	**23.88**	**23.88**	**23.88**
After 2 Cycles (angstroms)	**27.11**	**26.99**	**27.75**	**28.91**
After 4 Cycles (angstroms)	**27.87**	**27.19**	**29.07**	**32.66**

After four cycles of regeneration with both subcritical and supercritical water, there was also an increase in pore size; however, the change was less pronounced. This same trend was observed for loss of BET surface area in Table 4.2. Although the results were not conclusive, it is suspected that the largest loss of pore diameter and greatest loss of surface area occurred after the first adsorption stage when a small portion of phenol was chemisorbed.

The average pore size diameters for non-contaminated GAC samples subjected to regeneration are shown in Table 4.7. Surprisingly, there was not a significant increase in average pore diameter observed for any of the experiments. Furthermore, the effect of dissolved oxygen was insignificant. It is postulated that the increases in macropore volume observed in Table 4.5 were offset by increases in micropore and mesopore volume. Since the largest surface areas were associated with the micropore region, there was not an overall increase in average pore diameter.

Table 4.7 Average Pore Diameter of Non-Contaminated GAC after Regeneration.

Experiment	E	F	G
Regeneration Temperature (^{o}C)	*411*	*411*	*300*
Regeneration Pressure (MPa)	*26.2*	*26.2*	*12.4*
Dissolved Oxygen (mg/L)	*0*	*100*	*5*
Virgin GAC (angstroms)	**23.88**	**23.88**	**23.88**
After 2 Regenerations (angstroms)	**23.79**	**24.33**	**23.63**
After 4 Regenerations (angstroms)	**23.73**	**23.93**	**23.25**

The results in Table 4.7, when combined with the results in Table 4.3 and the data presented in Figure 4.8, also showed evidence of a mechanism known as pore deepening. Pore deepening occurs when there is an increase in surface area and total pore volume without an associated increase in average pore size. The opposite of pore deepening is pore drilling. Had pore drilling occurred, there would have been an increase in average pore size associated with the increase in volume. For the adsorption of small molecules, such as phenol, pore deepening is the preferred mechanism because there are no losses of adsorption sites.

4.7 Scanning Electron Microscopy

Selected samples of contaminated and non-contaminated GAC were examined under a scanning electron microscope (SEM). Although resolution was not good enough to view internal pores, it was sufficient to view magnified images of the surface of GAC. Figure 4.9 depicts a SEM photograph of virgin GAC, with an average BET surface area of 928 m^2/g, at a magnification of 100X. The irregular surface shows the numerous passageways that lead to the interior pore network. As shown in Figure 4.10, after four adsorption-regeneration cycles and a surface area of 522 m^2/g, the GAC surface was smoother and the pore entrances were not

as clearly defined. The lighter colored deposits on the surface of the GAC are likely decomposition products of phenol. Excessive burn-off or surface oxidation was not apparent. These observations were even more evident in Figures 4.11 and 4.12 that show the same samples at a magnification of 10000X.

Overall, the SEM photographs of phenol contaminated GAC after regeneration provided further evidence that pore plugging and/or chemisorption was responsible for the slight decrease in adsorption capacity over successive cycles.

Samples of non-contaminated GAC were also examined. Figure 4.13 depicts virgin GAC, with a BET surface area of 928 m^2/g, at a magnification of 100X. The same sample, after four regeneration stages with degassed SCW (Experiment E) and a BET surface area of 1075 m^2/g, is shown in Figure 4.14. Additional activation of the carbon surface was evident. In addition to the increase in surface area, there was a 14% increase in total pore volume. As with the contaminated GAC samples, there were no visible signs of excessive burn-off or surface oxidation.
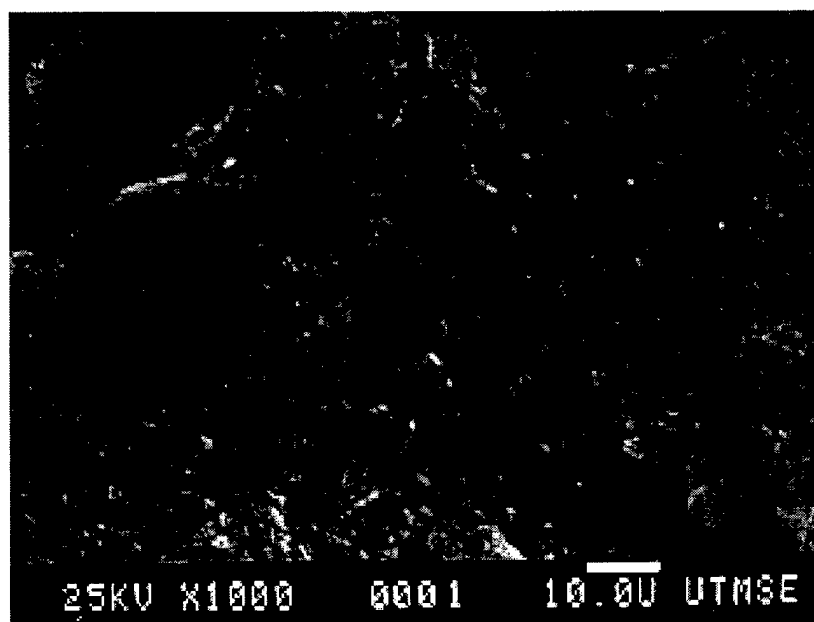
Figure 4.9 SEM Photograph (1000X) of Virgin GAC.
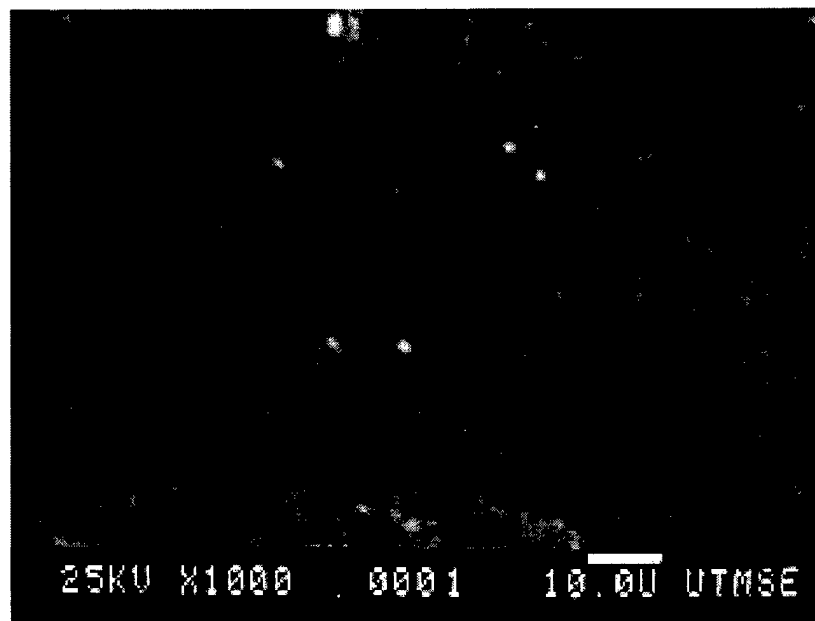
Figure 4.10 SEM Photograph (1000X) after Four Adsorption-Regeneration
Cycles (From Experiment A – SCW, 0 mg/L of Dissolved Oxygen).
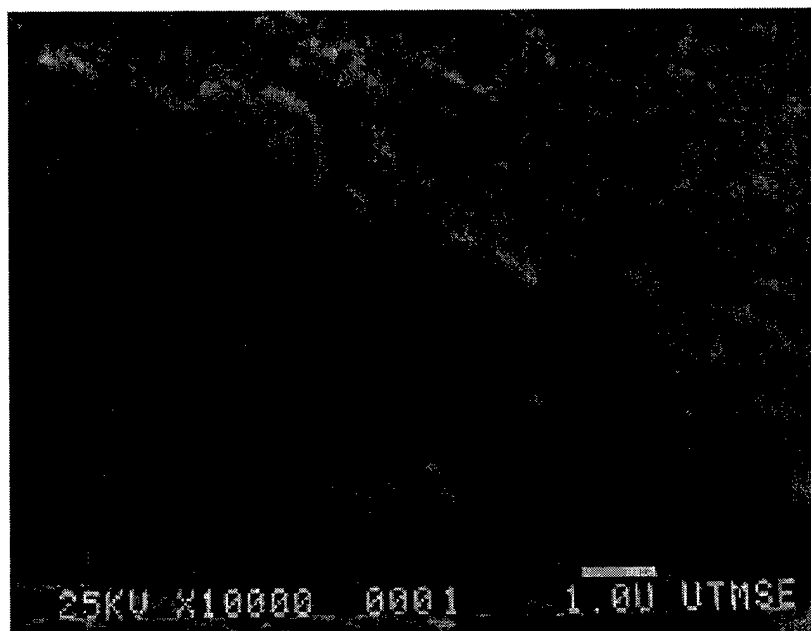
Figure 4.11 SEM Photograph (10000X) of Virgin GAC.
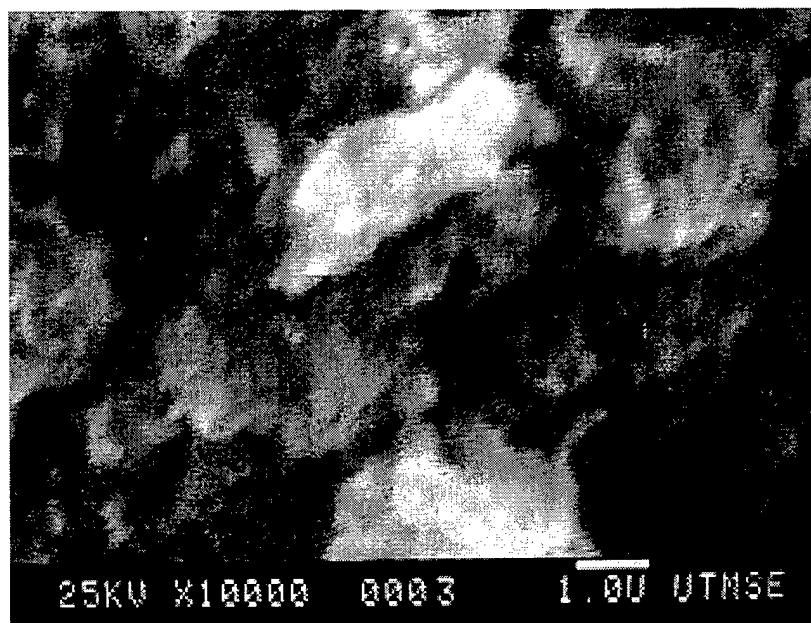
Figure 4.12 SEM Photograph (10000X) after Four Adsorption-Regeneration
Cycles (From Experiment A – SCW, 0 mg/L of Dissolved Oxygen).

60
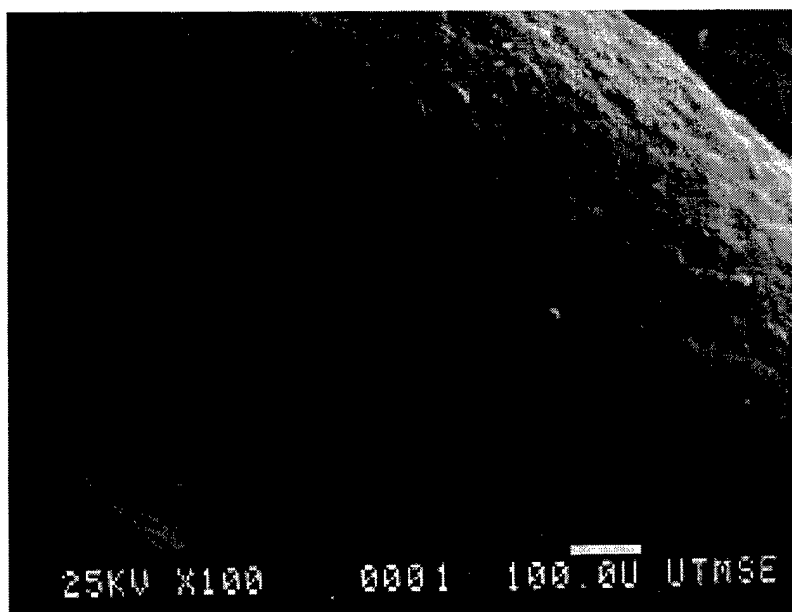
Figure 4.13 SEM Photograph (100X) of Virgin GAC.
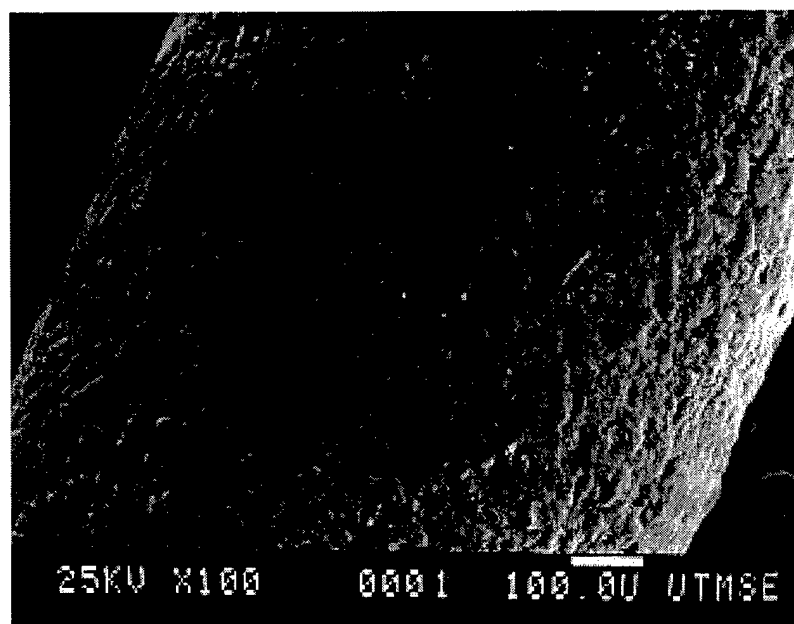
Figure 4.14 SEM Photograph (100X) of Non-Contaminated GAC after Four
Regenerations (From Experiment E – SCW, 0 mg/L of Dissolved Oxygen).

61

5.0 ENGINEERING SIGNIFICANCE

This study suggests that SCW is a viable option for the regeneration of spent GAC. While the results are specific to regeneration of NORIT Row 0.8 Supra GAC and removal of phenol, the process fundamentals are applicable to other activated carbon products and organic contaminants.

5.1 Benefits of using SCW to Regenerate Spent GAC

It is possible to remove organic contaminates from GAC at operating conditions less severe than the conventional 1000 °C normally used in industrial furnaces. Using SCW (411 °C and 26.2 MPa), 90% of the original adsorption capacity of GAC is restored after four adsorption-regeneration cycles. Dissolved oxygen concentrations as high as 100 mg/L are not inhibitory to the restoration of adsorption capacity and produce no noticeable impacts on surface area or pore size distribution. The two major benefits derived from the regeneration of contaminated GAC with SCW include: (a) reduced energy requirements; and (b) lower carbon losses.

5.2 GAC Recovery and Waste Treatment Using SCWO

One potential application of SCW regeneration involves a two-step process that includes both GAC recovery and waste treatment. In the first step, spent GAC is regenerated using SCW. In the second step, desorbed organic compounds are treated using supercritical water oxidation.

The regeneration process begins with the transfer of spent GAC from a carbon adsorption column to a regeneration vessel. The use of slurry pumps for this process is currently standard practice. After the regeneration vessel is filled with spent GAC, the system is pressurized with water to the desired operating conditions. Because dissolved oxygen does not inhibit the regeneration process, costly degassing operations are not required. The adsorbed organic compounds

are removed by passing SCW through the bed of spent carbon. The optimal temperature, pressure, and flow rate are a function of the adsorption characteristics of the adsorbate and need to be determined using pilot plant studies.

Treatment of the organic-laden stream of effluent leaving the vessel occurs in a follow-on reactor by injecting an oxidizing agent. On a commercial scale, it is likely that the residence time of the oxidation phase will be on the order of minutes. Under SCWO conditions, most organic material is rapidly broken down to CO_2, nitrogen gas, and water (Gloyna and Li, 1995). Since the end products of the SCWO process are non-toxic, no pollutants are released to the atmosphere. The treated water is then recycled back to the regeneration vessel.

At the conclusion of the regeneration stage, flow through the regeneration vessel is stopped. After depressurization, the regenerated GAC is transported back to the adsorption column via slurry pumps. To improve equipment utilization and eliminate filling and emptying downtime, a second regeneration vessel is recommended. With a two desorber configuration, one vessel is used for regeneration while the second vessel is in the filling mode.

6.0 CONCLUSIONS AND RECOMMENDATIONS

The regeneration of GAC using hydrothermal technology was evaluated. Spent GAC and non-contaminated GAC were subjected to multiple regeneration cycles using both supercritical and subcritical water that contained various amounts of dissolved oxygen. Conclusions of this study and recommendations for future work are presented.

6.1 Conclusions

- Regeneration of phenol contaminated GAC using SCW (411 °C and 26.2 MPa) was faster and more effective than regeneration with subcritical water (300 °C and 12.4 MPa). After four adsorption-regeneration cycles using SCW for regeneration, approximately 90% of the original adsorption capacity was restored. In contrast, only 67% of the original adsorption capacity was restored when using subcritical water for regeneration. The low density, viscosity, and surface tension of SCW resulted in an increased degree of penetration into micropores of GAC. Thus, more phenol was desorbed.

- Under SCW regeneration conditions (411 °C and 26.2 MPa), desorption was rapid. Approximately 60% and 90%, respectively, was removed in the first 20 and 60 minutes.

- Dissolved oxygen concentrations as high as 100 mg/L in SCW (411 °C and 26.2 MPa) were not detrimental to the restoration of adsorption capacity. Furthermore, dissolved oxygen produced no noticeable impacts on surface area or pore size distribution.

- The regeneration of spent GAC using SCW (411 °C and 26.2 MPa) is a viable alternative to the currently used thermal regeneration method. The advantages of SCW, as compared to conventional thermal processes, include lower energy requirements and lower carbon loss.

6.2 Recommendations

Recommendations for planning future work are provided below:

- Future studies must be conducted over a broader range of temperatures, pressures, and flow rates to determine optimal regeneration conditions.

- Additional studies that examine the regeneration of adsorbates contaminated with multiple adsorbates are needed since most industrial wastewater contains a heterogeneous mixture of organic compounds.

- Improvements in the design of the SCW heating system are recommended. The current design resulted in a heat-up phase that passed through subcritical temperatures. Future designs should incorporate a system that allows for the direct release of SCW to the spent carbon.

- Additional studies are needed to determine the feasibility of simultaneously conducting regeneration of spent GAC and destruction of organic contaminants using SCWO. In order to oxidize organic compounds in SCW these studies would need to use oxidants significantly greater than the 100 mg/L used in this study.

APPENDIX A: Adsorption Data

Adsorption Data for Experiment A

Regeneration Temperature: 411 °C
Regeneration Pressure: 26.2 MPa
Dissolved Oxygen: 0 mg/L

(Virgin)

Sample #	TOC (mg/L)	Volume (mL)	Phenol Adsorbed (g)
ADS091398-1	6582	(feed)	
-3	179.2	5	0.0422
-4	1000	10	0.0368
-5	1895	15	0.0309
-6	2522	20	0.0268
-7	2872	25	0.0245
-8	3378	30	0.0211
-9	3743	40	0.0375
-10	4279	50	0.0304
-11	4337	60	0.0296
-12	4899	70	0.0222
-13	5010	80	0.0207
-14	5320	90	0.0167
-15	5293	100	0.0170
-16	5445	110	0.0150
-17	5693	120	0.0117

(After one regeneration)

Sample #	TOC (mg/L)	Volume (mL)	Phenol Adsorbed (g)
ADS091898 -1	6654	(feed)	
-3	324.2	5	0.0418
-4	730.7	10	0.0391
-5	1618	15	0.0332
-6	2183	20	0.0295
-7	2763	25	0.0257
-8	3312	30	0.0220
-9	3802	40	0.0376
-10	4266	50	0.0315
-11	4544	60	0.0278
-12	4878	70	0.0234
-13	4986	80	0.0220
-14	5301	90	0.0179
-15	5395	100	0.0166
-16	5645	110	0.0133
-17	5689	120	0.0127

total phenol adsorbed (g)	0.3832

adsorptive capacity (g phenol/g carbon)	0.2546
change from virgin capacity (%)	N/A
regeneration capacity (%)	N/A

initial wt of carbon (g)	1.5051
wt of carbon after adsorption (g)	1.8310
Difference	0.3259

Final Regeneration TOC Prior to Adsorption Cycle (mg/L)	N/A

total phenol adsorbed (g)	0.3942

adsorptive capacity (g phenol/g carbon)	0.2619
change from virgin capacity (%)	2.8740
regeneration capacity (%)	103

wt of carbon before adsorption (g)	1.5186
wt of carbon after adsorption (g)	1.8530
Difference	0.3344

Final Regeneration TOC Prior to Adsorption Cycle (mg/L)	8.6

Adsorption Data for Experiment A (Continued)

Regeneration Temperature: 411 °C
Regeneration Pressure: 26.2 MPa
Dissolved Oxygen: 0 mg/L

(After two regenerations)

Sample #	TOC (mg/L)	Volume (mL)	Phenol Adsorbed (g)
ADS092998 -1	7328	(feed)	
-3	127.2	5	0.0475
-4	1637	10	0.0375
-5	3062	15	0.0281
-6	3991	20	0.0220
-7	4231	25	0.0204
-8	4584	30	0.0181
-9	4774	40	0.0337
-10	4914	50	0.0319
-11	5526	60	0.0238
-12	5526	70	0.0238
-13	5611	80	0.0227
-14	6088	90	0.0164
-15	6247	100	0.0143
-16	6596	110	0.0097
-17	6279	120	0.0138

total phenol adsorbed (g)	0.3636

adsorptive capacity (g phenol/g carbon)	0.2416
change from virgin capacity (%)	-5.1064
regeneration capacity (%)	95

wt of carbon before adsorption (g)	1.5269
wt of carbon after adsorption (g)	1.8820
Difference	0.3551

Final Regeneration TOC Prior to Adsorption Cycle (mg/L)	10.1

(After three regenerations)

Sample #	TOC (mg/L)	Volume (mL)	Phenol Adsorbed (g)
ADS100398 -1	6588	(feed)	
-3	40.2	5	0.0432
-4	361.3	10	0.0411
-5	1296	15	0.0349
-6	2184	20	0.0291
-7	2873	25	0.0245
-8	2937	30	0.0241
-9	3541	40	0.0402
-10	4342	50	0.0296
-11	4765	60	0.0241
-12	5151	70	0.0190
-13	5477	80	0.0147
-14	5591	90	0.0132
-15	5794	100	0.0105
-16	5845	110	0.0098
-17	5852	120	0.0097

total phenol adsorbed (g)	0.3675

adsorptive capacity (g phenol/g carbon)	0.2442
change from virgin capacity (%)	-4.0963
regeneration capacity (%)	96

wt of carbon before adsorption (g)	1.5367
wt of carbon after adsorption (g)	1.8450
Difference	0.3083

Final Regeneration TOC Prior to Adsorption Cycle (mg/L)	12.6

(After four regenerations)

Sample #	TOC (mg/L)	Volume (mL)	Phenol Adsorbed (g)
ADS110198 -1	8110	(feed)	
-3	2906	5	0.0343
-4	5400	10	0.0179
-5	5678	15	0.0160
-6	5771	20	0.0154
-7	5809	25	0.0152
-8	5852	30	0.0149
-9	5894	40	0.0292
-10	5956	50	0.0284
-11	5981	60	0.0281
-12	5950	70	0.0285
-13	6009	80	0.0277
-14	6259	90	0.0244
-15	6283	100	0.0241
-16	6303	110	0.0238
-17	6339	120	0.0234

total phenol adsorbed (g)	0.3515

adsorptive capacity (g phenol/g carbon)	0.2335
change from virgin capacity (%)	-8.2774
regeneration capacity (%)	92

wt of carbon before adsorption (g)	1.4761
wt of carbon after adsorption (g)	1.6078
Difference	0.1317

Final Regeneration TOC Prior to Adsorption Cycle (mg/L)	11.4

Adsorption Data for Experiment B

Regeneration Temperature: 411 °C
Regeneration Pressure: 26.2 MPa
Dissolved Oxygen: 5 mg/L

(Virgin)

Sample #	TOC (mg/L)	Volume (mL)	Phenol Adsorbed (g)
ADS071598-1	6956	(feed)	
-3	322.8	10	0.0875
-4	1232	20	0.0755
-5	2145	30	0.0635
-6	2794	40	0.0549
-7	3347	50	0.0476
-8	3774	60	0.0420
-9	4490	80	0.0651
-10	4839	100	0.0559
-11	5245	120	0.0452
-12	5467	140	0.0393
-13	5457	160	0.0396
-14	5829	180	0.0297
-15	5898	200	0.0279
-16	6002	220	0.0252
-17	6111	240	0.0223

loading of phenol (g phenol)	0.7211
adsorptive capacity (g phenol/g carbon)	0.2403
change from virgin capacity (%)	N/A
regeneration capacity (%)	N/A
wt of carbon before adsorption (g)	3.0012
wt of carbon after adsorption (g)	3.7013
Difference	0.7001
Final Regeneration TOC Prior to Adsorption Cycle (mg/L)	N/A

(After one regeneration)

Sample #	TOC (mg/L)	Volume (mL)	Phenol Adsorbed (g)
ADS071798 -1	6832	(feed)	
-3	454.7	10	0.0841
-4	1227	20	0.0740
-5	2127	30	0.0621
-6	2747	40	0.0539
-7	3020	50	0.0503
-8	3478	60	0.0443
-9	3958	80	0.0758
-10	4460	100	0.0626
-11	4646	120	0.0577
-12	5190	140	0.0433
-13	5369	160	0.0386
-14	5680	180	0.0304
-15	5802	200	0.0272
-16	5992	220	0.0222
-17	6192	240	0.0169

loading of phenol (g phenol)	0.7433
adsorptive capacity (g phenol/g carbon)	0.2477
change from virgin capacity (%)	3.0796
regeneration capacity (%)	103
wt of carbon before adsorption (g)	3.0021
wt of carbon after adsorption (g)	3.9480
Difference	0.9459
Final Regeneration TOC Prior to Adsorption Cycle (mg/L)	11.0

Adsorption Data for Experiment B (Continued)

Regeneration Temperature: 411 °C
Regeneration Pressure: 26.2 MPa
Dissolved Oxygen: 5 mg/L

(After two regenerations)

Sample #	TOC (mg/L)	Volume (mL)	Phenol Adsorbed (g)
ADS072198 -1	6784	(feed)	
-3	244.7	10	0.0863
-4	1765	20	0.0662
-5	2447	30	0.0572
-6	2966	40	0.0504
-7	3355	50	0.0452
-8	3730	60	0.0403
-9	4268	80	0.0664
-10	4802	100	0.0523
-11	5094	120	0.0446
-12	5407	140	0.0363
-13	5589	160	0.0315
-14	5765	180	0.0269
-15	5713	200	0.0283
-16	5906	220	0.0232
-17	5955	240	0.0219

loading of phenol (g phenol)	0.6770
adsorptive capacity (g phenol/g carbon)	0.2256
change from virgin capacity (%)	-6.1166
regeneration capacity (%)	94
wt of carbon before adsorption (g)	3.1345
wt of carbon after adsorption (g)	3.7915
Difference	0.6570
Final Regeneration TOC Prior to Adsorption Cycle (mg/L)	19.1

(After three regenerations)

Sample #	TOC (mg/L)	Volume (mL)	Phenol Adsorbed (g)
ADS072498 -1	6923	(feed)	
-3	133.9	10	0.0896
-4	858	20	0.0800
-5	1816	30	0.0674
-6	2824	40	0.0541
-7	3155	50	0.0497
-8	3512	60	0.0450
-9	4169	80	0.0727
-10	4712	100	0.0583
-11	5297	120	0.0429
-12	5898	140	0.0270
-13	5917	160	0.0265
-14	6149	180	0.0204
-15	6131	200	0.0209
-16	6253	220	0.0177
-17	6331	240	0.0156

loading of phenol (g phenol)	0.6879
adsorptive capacity (g phenol/g carbon)	0.2292
change from virgin capacity (%)	-4.6001
regeneration capacity (%)	95
wt of carbon before adsorption (g)	3.2281
wt of carbon after adsorption (g)	3.9130
Difference	0.6849
Final Regeneration TOC Prior to Adsorption Cycle (mg/L)	11.3

(After four regenerations)

Sample #	TOC (mg/L)	Volume (mL)	Phenol Adsorbed (g)
ADS072898 -1	7038	(feed)	
-3	132.9	10	0.0911
-4	719	20	0.0834
-5	1933	30	0.0674
-6	2549	40	0.0592
-7	3376	50	0.0483
-8	4409	60	0.0347
-9	4849	80	0.0578
-10	5541	100	0.0395
-11	5695	120	0.0354
-12	6056	140	0.0259
-13	6020	160	0.0269
-14	6181	180	0.0226
-15	6173	200	0.0228
-16	6432	220	0.0160
-17	6298	240	0.0195

loading of phenol (g phenol)	0.6505
adsorptive capacity (g phenol/g carbon)	0.2168
change from virgin capacity (%)	-9.7892
regeneration capacity (%)	90
wt of carbon before adsorption (g)	3.2743
wt of carbon after adsorption (g)	3.7640
Difference	0.4897
Final Regeneration TOC Prior to Adsorption Cycle (mg/L)	8.9

70

Adsorption Data for Experiment C

Regeneration Temperature: 411 °C
Regeneration Pressure: 26.2 MPa
Dissolved Oxygen: 100 mg/L

(Virgin)

Sample #	TOC (mg/L)	Volume (mL)	Phenol Adsorbed (g)
ADS082498-1	6752	(feed)	
-3	156.9	5	0.0435
-4	536	10	0.0410
-5	1115	15	0.0372
-6	1763	20	0.0329
-7	2539	25	0.0278
-8	3206	30	0.0234
-9	3718	40	0.0400
-10	4459	50	0.0303
-11	4747	60	0.0265
-12	5132	70	0.0214
-13	5322	80	0.0189
-14	5633	90	0.0148
-15	5927	100	0.0109
-16	5690	110	0.0140
-17	5633	120	0.0148

(After one regeneration)

Sample #	TOC (mg/L)	Volume (mL)	Phenol Adsorbed (g)
ADS082798 -1	6844	(feed)	
-3	23.1	5	0.0450
-4	164.6	10	0.0441
-5	380.2	15	0.0426
-6	1421	20	0.0358
-7	2217	25	0.0305
-8	2965	30	0.0256
-9	3631	40	0.0424
-10	4624	50	0.0293
-11	5097	60	0.0231
-12	5441	70	0.0185
-13	5548	80	0.0171
-14	5948	90	0.0118
-15	5944	100	0.0119
-16	6035	110	0.0107
-17	6048	120	0.0105

total phenol adsorbed (g)	0.3972
adsorptive capacity (g phenol/g carbon)	0.2643
change from virgin capacity (%)	N/A
regeneration capacity (%)	N/A
initial wt of carbon (g)	1.5027
wt of carbon after adsorption (g)	1.8840
Difference	0.3813
Final Regeneration TOC Prior to Adsorption Cycle (mg/L)	N/A

total phenol adsorbed (g)	0.3988
adsorptive capacity (g phenol/g carbon)	0.2654
change from virgin capacity (%)	0.4036
regeneration capacity (%)	100
wt of carbon before adsorption (g)	1.5045
wt of carbon after adsorption (g)	1.8650
Difference	0.3605
Final Regeneration TOC Prior to Adsorption Cycle (mg/L)	8.1

Adsorption Data for Experiment C (Continued)

Regeneration Temperature: 411 °C
Regeneration Pressure: 26.2 MPa
Dissolved Oxygen: 100 mg/L

(After two regenerations)

Sample #	TOC (mg/L)	Volume (mL)	Phenol Adsorbed (g)
ADS082998 -1	6680	(feed)	
-3	49.9	5	0.0437
-4	455	10	0.0411
-5	1184	15	0.0363
-6	1975	20	0.0310
-7	2533	25	0.0274
-8	3128	30	0.0234
-9	3822	40	0.0377
-10	4517	50	0.0285
-11	4888	60	0.0236
-12	5303	70	0.0182
-13	5492	80	0.0157
-14	5683	90	0.0132
-15	5801	100	0.0116
-16	6009	110	0.0089
-17	6044	120	0.0084

total phenol adsorbed (g)	0.3686

adsorptive capacity (g phenol/g carbon)	0.2453
change from virgin capacity (%)	-7.1965
regeneration capacity (%)	93

wt of carbon before adsorption (g)	1.4970
wt of carbon after adsorption (g)	1.8760
Difference	0.3790

Final Regeneration TOC Prior
to Adsorption Cycle (mg/L) | 18.7 |

(After three regenerations)

Sample #	TOC (mg/L)	Volume (mL)	Phenol Adsorbed (g)
ADS092898 -1	7222	(feed)	
-3	50.9	5	0.0473
-4	469.5	10	0.0445
-5	1745	15	0.0361
-6	2513	20	0.0311
-7	3423	25	0.0251
-8	3858	30	0.0222
-9	4655	40	0.0339
-10	5139	50	0.0275
-11	5494	60	0.0228
-12	5845	70	0.0182
-13	6136	80	0.0143
-14	6160	90	0.0140
-15	6390	100	0.0110
-16	6408	110	0.0107
-17	6572	120	0.0086

total phenol adsorbed (g)	0.3673

adsorptive capacity (g phenol/g carbon)	0.2444
change from virgin capacity (%)	-7.5394
regeneration capacity (%)	92

wt of carbon before adsorption (g)	1.5220
wt of carbon after adsorption (g)	1.8800
Difference	0.3580

Final Regeneration TOC Prior
to Adsorption Cycle (mg/L) | 11.4 |

(After four regenerations)

Sample #	TOC (mg/L)	Volume (mL)	Phenol Adsorbed (g)
ADS121598 -1	6945	(feed)	
-3	1225	5	0.0377
-4	1485	10	0.0360
-5	2198	15	0.0313
-6	2908	20	0.0266
-7	3799	25	0.0208
-8	4032	30	0.0192
-9	4778	40	0.0286
-10	5093	50	0.0244
-11	5372	60	0.0208
-12	5440	70	0.0199
-13	5697	80	0.0165
-14	5457	90	0.0196
-15	5704	100	0.0164
-16	5646	110	0.0171
-17	5904	120	0.0137

total phenol adsorbed (g)	0.3487

adsorptive capacity (g phenol/g carbon)	0.2320
change from virgin capacity (%)	-12.2224
regeneration capacity (%)	88

wt of carbon before adsorption (g)	1.5103
wt of carbon after adsorption (g)	1.8723
Difference	0.3620

Final Regeneration TOC Prior
to Adsorption Cycle (mg/L) | 9.1 |

Adsorption Data for Experiment D

Regeneration Temperature: 300 °C
Regeneration Pressure: 12.4 MPa
Dissolved Oxygen: 5 mg/L

(Virgin)

Sample #	TOC (mg/L)	Volume (mL)	Phenol Adsorbed (g)
ADS080298-1	6813	(feed)	
-3	31.6	10	0.0895
-4	386.9	20	0.0848
-5	1007	30	0.0766
-6	1931	40	0.0644
-7	2613	50	0.0554
-8	3425	60	0.0447
-9	4043	80	0.0731
-10	4535	100	0.0601
-11	4766	120	0.0540
-12	5314	140	0.0396
-13	5345	160	0.0387
-14	5617	180	0.0316
-15	5850	200	0.0254
-16	5855	220	0.0253
-17	6089	240	0.0191

(After one regeneration)

Sample #	TOC (mg/L)	Volume (mL)	Phenol Adsorbed (g)
ADS081198 -1	6873	(feed)	
-3	257	10	0.0873
-4	1100	20	0.0762
-5	2210	30	0.0615
-6	3092	40	0.0499
-7	3644	50	0.0426
-8	4194	60	0.0353
-9	4623	80	0.0594
-10	5056	100	0.0479
-11	5297	120	0.0416
-12	5659	140	0.0320
-13	5730	160	0.0302
-14	6011	180	0.0227
-15	6158	200	0.0189
-16	6262	220	0.0161
-17	6328	240	0.0144

total phenol adsorbed (g)	0.7823	total phenol adsorbed (g)	0.6361

adsorptive capacity (g phenol/g carbon)	0.2607	adsorptive capacity (g phenol/g carbon)	0.2119
change from virgin capacity (%)	N/A	change from virgin capacity (%)	-18.6922
regeneration capacity (%)	N/A	regeneration capacity (%)	81

initial wt of carbon (g)	3.0012	wt of carbon before adsorption (g)	3.0224
wt of carbon after adsorption (g)	3.7532	wt of carbon after adsorption (g)	3.5708
Difference	0.7520	Difference	0.5484

Final Regeneration TOC Prior to Adsorption Cycle (mg/L)	N/A	Final Regeneration TOC Prior to Adsorption Cycle (mg/L)	31.6

Adsorption Data for Experiment D (Continued)

Regeneration Temperature: 300 °C
Regeneration Pressure: 12.4 MPa
Dissolved Oxygen: 5 mg/L

(After two regenerations)

Sample #	TOC (mg/L)	Volume (mL)	Phenol Adsorbed (g)
ADS103198 -1	7480	(feed)	
-3	1798	5	0.0375
-4	2911	10	0.0301
-5	3029	15	0.0294
-6	3667	20	0.0252
-7	4645	25	0.0187
-8	5209	30	0.0150
-9	5438	40	0.0269
-10	5573	50	0.0252
-11	5663	60	0.0240
-12	5728	70	0.0231
-13	5860	80	0.0214
-14	6070	90	0.0186
-15	6258	100	0.0161
-16	6332	110	0.0151
-17	6339	120	0.0151

total phenol adsorbed (g)	0.3413

adsorptive capacity (g phenol/g carbon)	0.2268
change from virgin capacity (%)	-13.0017
regeneration capacity (%)	87

wt of carbon before adsorption (g)	1.5052
wt of carbon after adsorption (g)	1.7130
Difference	0.2078

Final Regeneration TOC Prior to Adsorption Cycle (mg/L)	12.7

(After three regenerations)

Sample #	TOC (mg/L)	Volume (mL)	Phenol Adsorbed (g)
ADS110398 -1	7430	(feed)	
-3	764.9	5	0.0440
-4	2105	10	0.0351
-5	2970	15	0.0294
-6	3927	20	0.0231
-7	4545	25	0.0190
-8	5208	30	0.0147
-9	5549	40	0.0248
-10	6123	50	0.0172
-11	6293	60	0.0150
-12	6341	70	0.0144
-13	6370	80	0.0140
-14	6592	90	0.0111
-15	6468	100	0.0127
-16	6592	110	0.0111
-17	6830	120	0.0079

total phenol adsorbed (g)	0.2935

adsorptive capacity (g phenol/g carbon)	0.1950
change from virgin capacity (%)	-25.2007
regeneration capacity (%)	75

wt of carbon before adsorption (g)	1.5134
wt of carbon after adsorption (g)	1.8140
Difference	0.3006

Final Regeneration TOC Prior to Adsorption Cycle (mg/L)	16.1

(After four regenerations)

Sample #	TOC (mg/L)	Volume (mL)	Phenol Adsorbed (g)
ADS0121698 -1	6945	(feed)	
-3	3457	5	0.0230
-4	3450	10	0.0231
-5	4201	15	0.0181
-6	4507	20	0.0161
-7	4324	25	0.0173
-8	4944	30	0.0132
-9	5033	40	0.0252
-10	5419	50	0.0201
-11	5366	60	0.0208
-12	5778	70	0.0154
-13	5592	80	0.0179
-14	5915	90	0.0136
-15	5476	100	0.0194
-16	6027	110	0.0121
-17	6502	120	0.0058

total phenol adsorbed (g)	0.2611

adsorptive capacity (g phenol/g carbon)	0.1735
change from virgin capacity (%)	-33.4452
regeneration capacity (%)	67

wt of carbon before adsorption (g)	1.5312
wt of carbon after adsorption (g)	1.8124
Difference	0.2812

Final Regeneration TOC Prior to Adsorption Cycle (mg/L)	15.4

74

APPENDIX B: Regeneration Data

Regeneration Data for Experiment A

Regeneration Temperature: 411 °C
Regeneration Pressure: 26.2 MPa
Dissolved Oxygen: 0 mg/L

(Regeneration # 1)

Sample #	TOC (mg/L)	Time (min)
GAC091798-1	15	0
-2	571.2	10
-3	1932	17
-4	631.2	24
-5	383	36
-6	112.5	48
-7	62.7	60
-8	34.9	85
-9	25.3	111
-10	18.5	137
-11	14.6	176
-12	15.4	215
-13	10.1	267
-14	8.6	300

(Regeneration # 2)

Sample #	TOC (mg/L)	Time (min)
GAC092098-1	11.4	0
-2	738.7	10
-3	1338	17
-4	753.9	24
-5	209.9	36
-6	60.8	48
-7	47	60
-8	30	85
-9	24.1	111
-10	18	137
-11	16	176
-12	15.3	215
-13	11.9	267
-14	10.1	300

(Regeneration # 3)

Sample #	TOC (mg/L)	Time (min)
GAC100298-1	18	0
-2	883.5	10
-3	846.9	17
-4	501.7	24
-5	230.8	36
-6	74.4	48
-7	44	60
-8	30.8	85
-9	24.7	111
-10	18.4	137
-11	17.3	176
-12	15	215
-13	13.2	267
-14	12.6	300

(Regeneration # 4)

Sample #	TOC (mg/L)	Time (min)
GAC101698-1	62.4	0
-2	1087	10
-3	1539	17
-4	334.3	24
-5	121.1	36
-6	49.6	48
-7	39.7	60
-8	26.6	85
-9	20.6	111
-10	17.7	137
-11	14.8	176
-12	14.2	215
-13	12.7	267
-14	11.4	300

Regeneration Data for Experiment B

Regeneration Temperature: 411 °C
Regeneration Pressure: 26.2 MPa
Dissolved Oxygen: 5 mg/L

(Regeneration # 1)

Sample #	TOC (mg/L)	Time (min)
GAC071698-1	161.2	0
-2	3545	10
-3	2435	17
-4	1092	24
-5	425.3	36
-6	166.2	48
-7	108.8	60
-8	59.6	85
-9	50.3	111
-10	35.3	137
-11	28.6	176
-12	17.6	215
-13	13.9	267
-14	11	300

(Regeneration # 2)

Sample #	TOC (mg/L)	Time (min)
GAC072098-1	16.1	0
-2	1993	10
-3	2291	17
-4	1045	24
-5	750.2	36
-6	201.5	48
-7	153.4	60
-8	80.5	85
-9	57.1	111
-10	42.4	137
-11	31.3	176
-12	29.4	215
-13	20	267
-14	19.1	300

(Regeneration # 3)

Sample #	TOC (mg/L)	Time (min)
GAC072398-1	159.7	0
-2	3685	10
-3	2136	17
-4	784.4	24
-5	553.9	36
-6	279	48
-7	99	60
-8	55.6	85
-9	39.6	111
-10	28.3	137
-11	23.1	176
-12	20.9	215
-13	18	267
-14	18.1	300

(Regeneration # 4)

Sample #	TOC (mg/L)	Time (min)
GAC072798-1	319.7	0
-2	947.4	10
-3	3193	17
-4	542.8	24
-5	182.7	36
-6	105.4	48
-7	59.8	60
-8	45	85
-9	50.3	111
-10	36.6	137
-11	30.3	176
-12	24.4	215
-13	19.4	267
-14	15.4	300

Regeneration Data for Experiment C

Regeneration Temperature: 411 °C
Regeneration Pressure: 26.2 MPa
Dissolved Oxygen: 100 mg/L

(Regeneration # 1)

Sample #	TOC (mg/L)	Time (min)
GAC082698-1	14.9	0
-2	287.9	10
-3	1740	17
-4	404.9	24
-5	196.2	36
-6	83.2	48
-7	54.7	60
-8	33.6	85
-9	29	111
-10	17.9	137
-11	14.2	176
-12	10.7	215
-13	10	267
-14	8.1	300

(Regeneration # 2)

Sample #	TOC (mg/L)	Time (min)
GAC082898-1	15.9	0
-2	402.2	10
-3	1379	17
-4	530.3	24
-5	249.8	36
-6	95.3	48
-7	63.2	60
-8	42.2	85
-9	42.6	111
-10	28.5	137
-11	18.8	176
-12	14.3	215
-13	15.8	267
-14	18.7	300

(Regeneration # 3)

Sample #	TOC (mg/L)	Time (min)
GAC083098-1	20.3	0
-2	902.4	10
-3	851	17
-4	526	24
-5	337.3	36
-6	106.5	48
-7	55.8	60
-8	43.3	85
-9	26.7	111
-10	40.6	137
-11	24.7	176
-12	16.3	215
-13	12.7	267
-14	11.4	300

(Regeneration # 4)

Sample #	TOC (mg/L)	Time (min)
GAC100198-1	14.8	0
-2	661.2	10
-3	1277	17
-4	364.6	24
-5	220.5	36
-6	92.6	48
-7	48.8	60
-8	28.2	85
-9	21.8	111
-10	19.2	137
-11	15.2	176
-12	13.1	215
-13	11.1	267
-14	9.1	300

Regeneration Data for Experiment D

Regeneration Temperature: 300 °C
Regeneration Pressure: 12.4 MPa
Dissolved Oxygen: 5 mg/L

(Regeneration # 1)

Sample #	TOC (mg/L)	Time (min)
GAC081098-1	17.5	0
-2	24	10
-3	1279	17
-4	1229	24
-5	490	36
-6	318.6	48
-7	270	60
-8	203.1	85
-9	148.4	111
-10	119.9	137
-11	79.7	176
-12	61.6	215
-13	42.5	267
-14	31.6	300

(Regeneration # 2)

Sample #	TOC (mg/L)	Time (min)
GAC082198-1	10.4	0
-2	135.9	10
-3	2239	17
-4	1028	24
-5	420.9	36
-6	225.2	48
-7	169.3	60
-8	118.3	85
-9	74.9	111
-10	49.8	137
-11	34	176
-12	23	215
-13	19.7	267
-14	12.7	300

(Regeneration # 3)

Sample #	TOC (mg/L)	Time (min)
GAC110298-1	185.3	0
-2	416.3	10
-3	1059	17
-4	189.9	24
-5	86.9	36
-6	62	48
-7	46.8	60
-8	27.6	85
-9	21.8	111
-10	17.2	137
-11	12.7	176
-12	10.6	215
-13	10.6	267
-14	16.1	300

(Regeneration # 4)

Sample #	TOC (mg/L)	Time (min)
GAC110698-1	44.2	0
-2	105	10
-3	1233	17
-4	122.3	24
-5	76.5	36
-6	55.2	48
-7	37.8	60
-8	28.2	85
-9	24	111
-10	22.3	137
-11	19.2	176
-12	15	215
-13	14	267
-14	15.4	300

APPENDIX C: BET Surface Area and Pore Size Distribution Data

BET Surface Area and Pore Size Distribution Data for Virgin GAC

Sample: Virgin Carbon # 1
BET Surface Area (m^2/g): 931
Average Pore Diameter (A): 23.99

Sample: Virgin Carbon # 2
BET Surface Area (m^2/g): 924.4
Average Pore Diameter (A): 23.88

Average Pore Diameter (A)	Pore Volume (cm^3/g)	Cumulative Pore Volume		Average Pore Diameter (A)	Pore Volume (cm^3/g)	Cumulative Pore Volume
19.8	0.007159	0.007159		19.8	0.007414	0.007414
20.7	0.0066	0.013759		20.7	0.006541	0.013955
21.7	0.007222	0.020981		21.6	0.006452	0.020407
23.3	0.012732	0.033713		23.2	0.013645	0.034052
25.9	0.010867	0.04458		25.6	0.008986	0.043038
28.3	0.006053	0.050633		28.1	0.010879	0.053917
30.1	0.004493	0.055126		30.9	0.005348	0.059265
32.9	0.017223	0.072349		34	0.02038	0.079645
38.1	0.053734	0.126083		38.8	0.047145	0.12679
43.5	0.008312	0.134395		43.5	0.008722	0.135512
49.1	0.008258	0.142653		49	0.007848	0.14336
56	0.007566	0.150219		55.9	0.007546	0.150906
64.6	0.008053	0.158272		64.6	0.008013	0.158919
75.2	0.007084	0.165356		75.3	0.006622	0.165541
86.2	0.005896	0.171252		86	0.005669	0.17121
98.2	0.006612	0.177864		98	0.006386	0.177596
111.1	0.004684	0.182548		110.7	0.004362	0.181958
123.6	0.005721	0.188269		123.3	0.005793	0.187751
139.5	0.006357	0.194626		140	0.006218	0.193969
157.8	0.005794	0.20042		157.4	0.004498	0.198467
177.2	0.006005	0.206425		176.6	0.006906	0.205373
200.8	0.007303	0.213728		203	0.00684	0.212213
229.5	0.006933	0.220661		228.9	0.004551	0.216764
258.3	0.005957	0.226618		256.1	0.006797	0.223561
287.5	0.005579	0.232197		290.3	0.005488	0.229049
321.8	0.006535	0.238732		321.6	0.00434	0.233389
361.9	0.005818	0.24455		357.9	0.005815	0.239204
403.7	0.005299	0.249849		405.9	0.005735	0.244939
456.1	0.006747	0.256596		462.7	0.006007	0.250946
523.1	0.005604	0.2622		531.1	0.004971	0.255917
584.3	0.003586	0.265786		597.7	0.003216	0.259133
640.6	0.00359	0.269376		651.1	0.002037	0.26117
740.4	0.004248	0.273624		696	0.001673	0.262843
950.6	0.003603	0.277227		771.2	0.003785	0.266628
1379.6	0.002562	0.279789		920.3	0.003346	0.269974
				1204.2	0.002122	0.272096

Total Volume:	0.279789
Micropores:	0.013759
Mesopores:	0.242837
Macropores:	0.023193

Total Volume:	0.272096
Micropores:	0.012993
Mesopores:	0.237953
Macropores:	0.02115

Average of Sample #1 and Sample #2
BET Surface Area (m2/g): 927.7
Average Pore Diamter (A): 23.94

Total Volume:	0.2759425
Micropores:	0.013376
Mesopores:	0.240395
Macropores:	0.0221715

81

BET Surface Area and Pore Size Distribution Data for Experiment A

Sample: Experiment A (After 2 cycles)

BET Surface Area (m^2/g): 706.4
Average Pore Diameter (A): 27.11

Average Pore Diameter (A)	Pore Volume (cm^3/g)	Cumulative Pore Volume
19.8	0.007236	0.007236
20.7	0.006583	0.013819
21.7	0.006266	0.020085
23.2	0.013061	0.033146
25.8	0.010853	0.043999
28.2	0.006315	0.050314
30	0.004703	0.055017
32.9	0.016319	0.071336
38	0.053861	0.125197
43.4	0.008263	0.13346
48.9	0.00744	0.1409
55.8	0.007381	0.148281
64.5	0.007599	0.15588
75.1	0.006548	0.162428
86	0.005506	0.167934
97.7	0.00627	0.174204
110.6	0.004795	0.178999
123.2	0.005466	0.184465
139.2	0.006749	0.191214
157.9	0.005619	0.196833
176.8	0.006261	0.203094
201.4	0.008123	0.211217
229.7	0.006157	0.217374
256.7	0.006761	0.224135
288.4	0.006616	0.230751
322.1	0.006254	0.237005
359.8	0.00661	0.243615
405.3	0.006495	0.25011
456.4	0.005811	0.255921
511.5	0.005084	0.261005
598.2	0.008907	0.269912
778	0.008055	0.277967
1141.2	0.004985	0.282952

Total Volume:	0.282952
Micropores:	0.013819
Mesopores:	0.242102
Macropores:	0.027031

Sample: Experiment A (After 4 cycles)

BET Surface Area (m^2/g): 522.2
Average Pore Diameter (A): 27.87

Average Pore Diameter (A)	Pore Volume (cm^3/g)	Cumulative Pore Volume
19.8	0.006106	0.006106
20.7	0.006107	0.012213
21.7	0.005744	0.017957
23.2	0.011751	0.029708
25.8	0.010031	0.039739
28.1	0.005757	0.045496
30.4	0.006967	0.052463
33.7	0.013815	0.066278
38.3	0.045194	0.111472
43.4	0.009198	0.12067
48.9	0.006319	0.126989
55.8	0.006022	0.133011
64.5	0.006	0.139011
75.1	0.005001	0.144012
86	0.004196	0.148208
97.7	0.004518	0.152726
110.5	0.003297	0.156023
123.2	0.003775	0.159798
138.9	0.004312	0.16411
157.1	0.00381	0.16792
176.2	0.004033	0.171953
200.9	0.005149	0.177102
225.4	0.002287	0.179389
251.9	0.006623	0.186012
305.7	0.00712	0.193132
378.9	0.00758	0.200712
489.7	0.009124	0.209836
694.9	0.008911	0.218747
1085.6	0.008132	0.226879

Total Volume:	0.226879
Micropores:	0.012213
Mesopores:	0.188499
Macropores:	0.026167

BET Surface Area and Pore Size Distribution Data for Experiment C

Sample: Experiment C (After 2 cycles)
BET Surface Area (m^2/g): 608.9
Average Pore Diameter (A): 27.75

Average Pore Diameter (A)	Pore Volume (cm^3/g)	Cumulative Pore Volume
19.8	0.006853	0.006853
20.7	0.006229	0.013082
21.7	0.005981	0.019063
23.2	0.012434	0.031497
25.8	0.01026	0.041757
28.2	0.005767	0.047524
30	0.004732	0.052256
33	0.016271	0.068527
38.1	0.052168	0.120695
43.4	0.007696	0.128391
48.9	0.006385	0.134776
55.8	0.006266	0.141042
64.5	0.00647	0.147512
75.1	0.005548	0.15306
86	0.004739	0.157799
97.7	0.005341	0.16314
110.6	0.00419	0.16733
123.2	0.0047	0.17203
138.9	0.005561	0.177591
157.1	0.00483	0.182421
176	0.005611	0.188032
200.7	0.006904	0.194936
228.5	0.005178	0.200114
255.4	0.00574	0.205854
287.4	0.005764	0.211618
320.4	0.004918	0.216536
358.4	0.006292	0.222828
404.4	0.004766	0.227594
453.6	0.005533	0.233127
517.3	0.005269	0.238396
617	0.008674	0.24707
826.6	0.008161	0.255231
1244.2	0.00716	0.262391

Total Volume:	0.262391
Micropores:	0.013082
Mesopores:	0.220045
Macropores:	0.029264

Sample: Experiment C (After 4 cycles)
BET Surface Area (m^2/g): 528.4
Average Pore Diameter (A): 29.07

Average Pore Diameter (A)	Pore Volume (cm^3/g)	Cumulative Pore Volume
19.8	0.005749	0.005749
20.7	0.005756	0.011505
21.7	0.005557	0.017062
23.2	0.011135	0.028197
25.8	0.009539	0.037736
28.1	0.005414	0.04315
30.4	0.006715	0.049865
33.7	0.014625	0.06449
38.3	0.044625	0.109115
43.4	0.007345	0.11646
48.9	0.006519	0.122979
55.8	0.006359	0.129338
64.5	0.006556	0.135894
75.1	0.00566	0.141554
86	0.004728	0.146282
97.7	0.005266	0.151548
110.5	0.003978	0.155526
123.2	0.00478	0.160306
139.1	0.005214	0.16552
156.9	0.004641	0.170161
176.2	0.005335	0.175496
200.5	0.00642	0.181916
228.4	0.004933	0.186849
255.5	0.005386	0.192235
287	0.00512	0.197355
320.3	0.004852	0.202207
357.8	0.005186	0.207393
402.1	0.004909	0.212302
442.7	0.003063	0.215365
516.4	0.011126	0.226491
714.7	0.009535	0.236026
1104.5	0.006512	0.242538

Total Volume:	0.242538
Micropores:	0.011505
Mesopores:	0.20386
Macropores:	0.027173

BET Surface Area and Pore Size Distribution Data for Experiment D

Sample: Experiment D (After 2 cycles)
BET Surface Area (m²/g): 568.5
Average Pore Diameter (A): 28.91

Sample: Experiment D (After 4 cycles)
BET Surface Area (m²/g): 370.5
Average Pore Diameter (A): 32.66

Average Pore Diameter (A)	Pore Volume (cm³/g)	Cumulative Pore Volume		Average Pore Diameter (A)	Pore Volume (cm³/g)	Cumulative Pore Volume
19.8	0.006183	0.006183		19.8	0.005073	0.005073
20.7	0.005814	0.011997		20.7	0.004972	0.010045
21.7	0.006523	0.01852		21.7	0.00486	0.014905
23.4	0.010537	0.029057		23.2	0.010127	0.025032
25.9	0.010201	0.039258		25.8	0.008766	0.033798
28.4	0.00617	0.045428		28.2	0.005148	0.038946
30.3	0.003916	0.049344		30.2	0.005228	0.044174
33.3	0.018914	0.068258		33.3	0.015	0.059174
38.6	0.045575	0.113833		38.2	0.042896	0.10207
43.5	0.007686	0.121519		43.4	0.007129	0.109199
49	0.006835	0.128354		48.9	0.006444	0.115643
55.8	0.006774	0.135128		55.7	0.006284	0.121927
64.6	0.006923	0.142051		64.4	0.00635	0.128277
75.1	0.00607	0.148121		75	0.005362	0.133639
86	0.005082	0.153203		85.8	0.00432	0.137959
97.8	0.005667	0.15887		97.5	0.004798	0.142757
110.6	0.00423	0.1631		110.3	0.00364	0.146397
123.3	0.005034	0.168134		122.8	0.003994	0.150391
139.3	0.0057	0.173834		138.4	0.004202	0.154593
157	0.004722	0.178556		156.6	0.004202	0.158795
176.3	0.006107	0.184663		175.5	0.004494	0.163289
201	0.006402	0.191065		199.8	0.005544	0.168833
227.7	0.005543	0.196608		227.4	0.004114	0.172947
255.8	0.006116	0.202724		254.2	0.00475	0.177697
286.5	0.005158	0.207882		285.2	0.004368	0.182065
319.2	0.005756	0.213638		318.8	0.004507	0.186572
358.7	0.005819	0.219457		356.4	0.004217	0.190789
401.5	0.00476	0.224217		398.5	0.004221	0.19501
452.9	0.006254	0.230471		442.1	0.003243	0.198253
520.3	0.005221	0.235692		517.5	0.009385	0.207638
587.4	0.003725	0.239417		701.3	0.007747	0.215385
647.4	0.002466	0.241883		1051.1	0.00526	0.220645
692.2	0.001368	0.243251				
766.7	0.004178	0.247429				
935.1	0.003805	0.251234				
1264.1	0.002543	0.253777				

Total Volume:	0.220645
Micropores:	0.010045
Mesopores:	0.188208
Macropores:	0.022392

Total Volume:	0.253777
Micropores:	0.011997
Mesopores:	0.218474
Macropores:	0.023306

84

BET Surface Area and Pore Size Distribution Data for Experiment E

Sample: Experiment E (SCW x 2, degassed)
BET Surface Area (m²/g): 1036
Average Pore Diameter (A): 23.79

Average Pore Diameter (A)	Pore Volume (cm³/g)	Cumulative Pore Volume
19.8	0.008825	0.008825
20.7	0.007622	0.016447
21.6	0.007076	0.023523
23.2	0.015582	0.039105
25.9	0.012844	0.051949
28.5	0.00791	0.059859
30.6	0.004949	0.064808
33.6	0.021487	0.086295
38.8	0.054222	0.140517
43.5	0.008988	0.149505
49	0.007543	0.157048
56	0.007309	0.164357
64.8	0.007344	0.171701
75.5	0.006579	0.17828
86.4	0.005423	0.183703
98.3	0.006543	0.190246
111.6	0.004793	0.195039
123.8	0.005238	0.200277
139.6	0.007186	0.207463
158.4	0.005765	0.213228
177.1	0.006505	0.219733
201.7	0.008547	0.22828
229.4	0.005973	0.234253
256.1	0.007554	0.241807
288.7	0.006841	0.248648
321.7	0.006249	0.254897
358.7	0.006681	0.261578
404.7	0.006959	0.268537
461	0.00662	0.275157
527.2	0.005748	0.280905
594.2	0.003799	0.284704
654.4	0.002964	0.287668
718.5	0.002538	0.290206
812.8	0.004139	0.294345
989.6	0.003926	0.298271
1348.2	0.002958	0.301229

Total Volume:	0.301229
Micropores:	0.016447
Mesopores:	0.25871
Macropores:	0.026072

Sample: Experiment E (SCW x 4, degassed)
BET Surface Area (m²/g): 1075
Average Pore Diameter (A): 23.73

Average Pore Diameter (A)	Pore Volume (cm³/g)	Cumulative Pore Volume
19.8	0.009162	0.009162
20.7	0.008341	0.017503
21.8	0.009946	0.027449
23.4	0.014022	0.041471
25.9	0.013636	0.055107
28.5	0.007959	0.063066
30.3	0.004652	0.067718
33.3	0.022738	0.090456
38.7	0.05745	0.147906
43.6	0.009364	0.15727
49.1	0.007877	0.165147
56	0.007666	0.172813
64.8	0.007678	0.180491
75.5	0.006894	0.187385
86.1	0.005391	0.192776
97.7	0.00671	0.199486
111	0.005198	0.204684
123.6	0.005539	0.210223
139.4	0.006952	0.217175
157.7	0.005937	0.223112
176.7	0.006724	0.229836
201.4	0.008589	0.238425
228.7	0.005912	0.244337
256.5	0.008744	0.253081
289.5	0.005792	0.258873
318.9	0.00608	0.264953
357.2	0.007856	0.272809
406.7	0.008132	0.280941
463.1	0.006553	0.287494
528	0.006747	0.294241
598.8	0.004445	0.298686
659	0.003145	0.301831
704.6	0.001267	0.303098
777.3	0.004993	0.308091
954.3	0.004693	0.312784
1301	0.00312	0.315904

Total Volume:	0.315904
Micropores:	0.017503
Mesopores:	0.269991
Macropores:	0.02841

BET Surface Area and Pore Size Distribution Data for Experiment F

Sample: Experiment F (SCW x 2, H$_2$O$_2$)
BET Surface Area (m^2/g): 1046
Average Pore Diameter (A): 24.33

Average Pore Diameter (A)	Pore Volume (cm^3/g)	Cumulative Pore Volume
19.8	0.008803	0.008803
20.7	0.0074446	0.0162476
21.6	0.007259	0.0235066
23.2	0.01653	0.0400366
25.9	0.01358	0.0536166
28.5	0.008261	0.0618776
30.4	0.005118	0.0669956
33.4	0.023376	0.0903716
38.7	0.056696	0.1470676
43.5	0.01006	0.1571276
49	0.008651	0.1657786
55.8	0.008294	0.1740726
64.5	0.008684	0.1827566
75.3	0.00761	0.1903666
86.3	0.006082	0.1964486
98	0.007138	0.2035866
111.1	0.005508	0.2090946
123.8	0.00595	0.2150446
139.9	0.007618	0.2226626
158.2	0.005758	0.2284206
177	0.007428	0.2358486
201.7	0.008032	0.2438806
228.9	0.00697	0.2508506
257.5	0.007488	0.2583386
287.6	0.005823	0.2641616
320.7	0.007926	0.2720876
360.4	0.006347	0.2784346
403.8	0.007495	0.2859296
462.7	0.007962	0.2938916
525.5	0.005491	0.2993826
573.7	0.002745	0.3021276
622.6	0.004818	0.3069456
710.4	0.006039	0.3129846
789.1	0.000772	0.3137566
858	0.004656	0.3184126
1037.6	0.004486	0.3228986
1387.8	0.003224	0.3261226

Total Volume:	0.3261226
Micropores:	0.0162476
Mesopores:	0.277644
Macropores:	0.032231

Sample: Experiment F (SCW x 4, H$_2$O$_2$)
BET Surface Area (m^2/g): 1034
Average Pore Diameter (A): 23.93

Average Pore Diameter (A)	Pore Volume (cm^3/g)	Cumulative Pore Volume
19.8	0.008807	0.008807
20.7	0.00762	0.016427
21.8	0.009007	0.025434
23.4	0.013492	0.038926
25.9	0.012609	0.051535
28.4	0.007588	0.059123
30.2	0.004299	0.063422
33.2	0.021256	0.084678
38.6	0.057133	0.141811
43.6	0.009281	0.151092
49	0.007715	0.158807
55.8	0.007553	0.16636
64.6	0.008016	0.174376
75.3	0.006616	0.180992
86.1	0.006	0.186992
98.1	0.006557	0.193549
110.9	0.004921	0.19847
123.4	0.005487	0.203957
139.3	0.007117	0.211074
157.6	0.00557	0.216644
176.6	0.007257	0.223901
201.4	0.007439	0.23134
228	0.006817	0.238157
256.7	0.00752	0.245677
287.3	0.00593	0.251607
315.8	0.006518	0.258125
358.2	0.007337	0.265462
403.2	0.006323	0.271785
457.4	0.007757	0.279542
524.8	0.005837	0.285379
593	0.005219	0.290598
654.7	0.002491	0.293089
712.6	0.00345	0.296539
816.5	0.004802	0.301341
991.8	0.004341	0.305682
1354.8	0.003382	0.309064

Total Volume:	0.309064
Micropores:	0.016427
Mesopores:	0.263115
Macropores:	0.029522

BET Surface Area and Pore Size Distribution Data for Experiment G

Sample: Experiment G (Subcritical x 2)
BET Surface Area (m^2/g): 1034
Average Pore Diameter (A): 23.63

Average Pore Diameter (A)	Pore Volume (cm^3/g)	Cumulative Pore Volume
19.8	0.009044	0.009044
20.7	0.006803	0.015847
21.6	0.00747	0.023317
23.2	0.017559	0.040876
25.9	0.013236	0.054112
28.5	0.007664	0.061776
30.3	0.004411	0.066187
33.3	0.021458	0.087645
38.7	0.057551	0.145196
43.6	0.009404	0.1546
48.9	0.007122	0.161722
55.7	0.006796	0.168518
64.4	0.007189	0.175707
75.1	0.006098	0.181805
85.8	0.005172	0.186977
97.6	0.00602	0.192997
123	0.005475	0.198472
139.2	0.006296	0.204768
157	0.005262	0.21003
175.8	0.006439	0.216469
200.5	0.007696	0.224165
228.1	0.006131	0.230296
255.3	0.006491	0.236787
285	0.005619	0.242406
317.8	0.006766	0.249172
356.4	0.00602	0.255192
400.3	0.006528	0.26172
455.9	0.006204	0.267924
516.8	0.004689	0.272613
581.4	0.004198	0.276811
646.1	0.002803	0.279614
703	0.0023	0.281914
795.6	0.004344	0.286258

Total Volume:	0.286258
Micropores:	0.015847
Mesopores:	0.252077
Macropores:	0.018334

Sample: Experiment G (Subcritical x 4)
BET Surface Area (m^2/g): 1047
Average Pore Diameter (A): 23.25

Average Pore Diameter (A)	Pore Volume (cm^3/g)	Cumulative Pore Volume
19.8	0.009531	0.009531
20.7	0.007926	0.017457
21.6	0.007828	0.025285
23.2	0.017566	0.042851
25.9	0.012873	0.055724
28.4	0.007833	0.063557
30.2	0.00456	0.068117
33.2	0.022698	0.090815
38.7	0.057682	0.148497
43.5	0.008295	0.156792
49	0.006731	0.163523
55.8	0.006691	0.170214
64.6	0.006566	0.17678
75	0.005914	0.182694
85.8	0.004835	0.187529
97.5	0.00577	0.193299
110.6	0.0046	0.197899
123.1	0.00489	0.202789
139.1	0.006668	0.209457
156.9	0.004207	0.213664
175.4	0.007498	0.221162
201.7	0.006776	0.227938
227.1	0.005689	0.233627
255.5	0.007394	0.241021
286.4	0.004989	0.24601
315.5	0.005675	0.251685
351.6	0.006288	0.257973
394.5	0.005973	0.263946
447.1	0.006179	0.270125
511.2	0.00547	0.275595
575.6	0.003564	0.279159
631.1	0.002629	0.281788
680.8	0.001879	0.283667
760.6	0.004453	0.28812
934.3	0.004284	0.292404
1288.3	0.003367	0.295771

Total Volume:	0.295771
Micropores:	0.017457
Mesopores:	0.252668
Macropores:	0.025646

REFERENCES

Bansal, R.; Donnet, J.; Stoeckli, F. *Active Carbon;* Marcel Dekker, Inc.: New York, 1988.

Barrett, H.; Joyner, L.; Halenda, P. The Determination of Pore Volume and Area Distributions in Porous Substances. *J. Amer. Chem. Soc.*, 1951, *73*, pp. 373-380.

Chakravorti, R.; Weber, T. A Comprehensive Study of the Adsorption of Phenol in a Packed Bed of Activated Carbon. *AIChE Symposium Series* 1975, *71* (151), pp. 392-403.

Cheremisinoff, P.; Morresi, A. Carbon Adsorption Applications. *Carbon Adsorption Handbook*; Cheremisinoff, P.; Ellerbusch, F., Eds.; Ann Arbor Science: Ann Arbor, MI, 1978, pp.1-53.

Cookson, J. Adsorption Mechanisms: The Chemistry of Organic Adsorption on Activated Carbon. *Carbon Adsorption Handbook*; Cheremisinoff, P.; Ellerbusch, F., Eds.; Ann Arbor Science: Ann Arbor, MI, 1978, pp. 241-279.

Cooney, D. *Adsorption Design for Wastewater Treatment*; Lewis Publishers: New York, 1999.

De Filippi, R., Krukonis, R.; Modell, M. Supercritical Fluid Regeneration of Activated Carbon for Adsorption of Pesticides. Report: EPA-600/2-80054, March 1980.

Droste, R. *Theory and Practice of Water and Wastewater Treatment*; John Wiley & Sons, Inc.: New York, 1997.

Ferro, M.; Utera, E.; Rivera, J.; Moreno, C. Regeneration of Activated Carbons Exhausted with Chlorophenols. *Carbon* 1993, *31,* pp. 857-862.

Gitchel, W.; Meidl, J.; Berndt, C. Characteristics of Active Carbon Regenerated by Wet Oxidation. *AIChE Symposium Series* 1980, *76* (192), pp.51-59.

Gloyna, E.; Li, L. Supercritical Water Oxidation Research and Development Update. *Environ. Prog.* 1995, *14* (3), pp. 182-192.

Greenberg, A.; Clesceri, L.; Eaton, A. *Standard Methods for Examination of Water and Wastewater –18th Edition*; American Public Health Association: Washington, D.C., 1992.

Himmelstein, K.; Fox, R.; Winter, T. In Place Regeneration of Activated Carbon. *Chem. Eng. Prog.* 1973, *69*, pp. 65-69.

Hutchenson, K.; Roebers, J.; Thies, M. Fractionation of Petroleum Pitch by Supercritical Fluid Extraction. *Carbon* 1991, *29* (2), pp. 215-223.

Hutchins, R. Costs of Thermal Regeneration. *AIChE Symposium Series* 1991, *71* (151), pp. 423-431.

Jankowska, H.; Swiatkowski, A.; Choma, J. *Active Carbon*; Ellis Horwood Limited: Chichester, England, 1991.

Johnston, K. Safer Solutions for Chemist. *Nature* 1994, *368*, pp. 187-188.

Josephson, J. Supercritical Fluids. *Environ. Sci. Technol.* 1982, *16* (10), pp. 548A-551A.

Knopp, P.; Gitchel, J.; Meidl, J.; Berndt, C. Wet Oxidation Regeneration. *Carbon Adsorption Handbook*; Cheremisinoff, P.; Ellerbusch, F., Eds.; Ann Arbor Science: Ann Arbor, MI, 1978, pp. 539-625.

Leng, C.; Pinto, N. An Investigation of the Mechanisms of Chemical Regeneration of Activated Carbon. *Ind. Eng. Chem.* 1996, *35*, pp. 2024-2031.

Lyman, W. Applicability of Carbon Adsorption to the Treatment of Hazardous Industrial Wastes. *Carbon Adsorption Handbook*; Cheremisinoff, P.; Ellerbusch, F., Eds.; Ann Arbor Science: Ann Arbor, MI, 1978, pp. 131-165.

Magne, P.; Walker, P. Phenol Adsorption on Activated Carbons: Application to the Regeneration of Activated Carbons Polluted with Phenol. *Carbon* 1986, *24* (2), pp. 101-107.

McGinnis, F. Thermal Regeneration of Activated Carbon. *Pollution Eng.* 1994, *16* (1), pp. 40-42.

McHugh, M.; Krukonis, V. *Supercritical Fluid Extraction: Principals and Practice*; Butterworth-Heinemann: Boston, MA, 1994.

Micromeritics, *ASAP 2010 Accelerated Surface Area and Porisimetry System Operators Manual*, July 1995, pp. C1-C43.

Modell, M.; DeFillipi, R.; Krukonis, V. Regeneration of Activated Carbon with Supercritical Carbon Dioxide. *Activated Carbon Adsorption of Organics from the Aqueous Phase*; Suffet, I. H.;McGuire, M. J., Eds.; Ann Arbor Science: Ann Arbor, MI, 1980; Vol. 1, pp. 447-461.

Mundale, V.; Joglekar, A.; Joshi, J. Regeneration of Spent Activated Carbon by Wet Air Oxidation. *J.. Canadian Chem. Eng.* 1991, *69*, pp. 1149-1159.

Pahl, R.; Mayhan, K.; Bertrand, G. Organic Desorption From Carbon II: The Effect of Solvent in the Desorption of Phenol From Wet Carbon. *Water Res.* 1973, *7*, pp. 1309-1322.

Patrick, J. *Porosity in Carbons*; Halsted Press: New York, 1995.

Randtke, S.D. and Snoeyink, V. Evaluating GAC Adsorptive Capacity. *J. of AWWA*, 1983, *75* (8), pp. 406-413.

Recasens, F.; McCoy, B.; Smith, J. Desorption Processes: Supercritical Fluid Regeneration of Activated Carbon. *AIChE Symposium Series* 1989, *35* (6), pp. 951-958.

Salvador, F.; Sanchez, C.; Merchan, M. Regeneration of an Activated Carbon with Supercritical Water. *The European Carbon Conference "Carbon 96"* at Newcastle, U.K. (July 1996).

Salvador, F.; Sanchez, C. A New Method for Regenerating Activated Carbon by Thermal Desorption with Liquid Water Under Subcritical Conditions. *Carbon* 1996, *34* (4), pp. 511-516.

Sawyer, C.; McCarty, P.; Parkin, G. *Chemistry for Environmental Engineering*; McGraw-Hill Inc.: New York, 1994.

Shaw, R.; Brill, T.; Clifford, A.; Eckert, C.; Ulrich, F. Supercritical Water: A Medium for Chemistry. *Chem. Eng. News* 1991, *69*, pp. 26-39.

Smisek, M.; Cerny, S. *Active Carbon: Manufacture, Properties, and Applications*; Elsevier Publishing Company: Czechoslovakia, 1970.

Smithson G. Regeneration of Activated Carbon: Thermal, Chemical, Solvent Vacuum, and Miscellaneous Regeneration Techniques. *Carbon Adsorption Handbook*; Cheremisinoff, P.; Ellerbusch, F., Eds.; Ann Arbor Science: Ann Arbor, MI, 1978, pp. 879-903.

Srinivasan, M.; Smith, J.; McCoy B. Supercritical Fluid Desorption From Activated Carbon. *Chem. Eng. Sci.* 1990, *45* (7), pp. 1885-1895.

Tan, C.; Liou, D. Desorption of Ethyl Acetate from Activated Carbon by Supercritical Carbon Dioxide. *Ind. Eng. Chem. Res.* 1988, *27*, pp. 988-991.

Urano, K.; Yamamoto, E.; Takeda, H. Regeneration Rates of Granular Activated Carbons Containing Adsorbed Organic Matter. *Ind. Eng. Chem. Proc. Des. Dev.* 1982, *21*, pp. 180-185.

U.S. Environmental Protection Agency, Process Design Manual for Carbon Adsorption (October 1973).

Van Vliet, B. The Regeneration of Activated Carbon. *J. S. Afr. Inst. Min. Metalt.* 1991, *91* (5), pp. 159-167.

Weber, W.; Van Vliet, B. Fundamental Concepts for Applications of Activated Carbon in Water and Wastewater Treatment. *Activated Carbon Adsorption of Organics from the Aqueous Phase*; Suffet, I. H.;McGuire, M. J., Eds.; Ann Arbor Science: Ann Arbor, MI, 1980; Vol. 1, pp. 15-41.

Wigmans, T. Industrial Aspects of Production and Use of Activated Carbons. *Carbon*, 1989, *27* (1), pp. 13-22.

Zanitsch, R.; Stenzel, M. Economics of Granular Activated Carbon Water and Wastewater Treatment Systems. *Carbon Adsorption Handbook*; Cheremisinoff, P.; Ellerbusch, F., Eds.; Ann Arbor Science: Ann Arbor, MI, 1978, pp. 215-239.

VITA

Michael D. Sufnarski was born in Wells, Vermont on January 25, 1968, the son of Frances and Stanley Sufnarski. After graduating from Granville High School, Granville, New York in 1986, he entered the United States Military Academy at West Point, New York. In May 1990, he received the degree of Bachelor of Science and was commissioned as a Second Lieutenant in the United States Army. His first assignment was with the 27th Engineer Battalion (Combat) (Airborne) at Fort Bragg, North Carolina where he served as Platoon Leader, Company Executive Officer and Battalion Air Officer. After completing the Engineer Officer Advanced Course in January 1995, CPT Sufnarski was assigned to Fort Stewart, Georgia where he served as Brigade Plans Officer for the 24th Infantry Division Engineer Brigade and Assistant Brigade Engineer for 2nd Brigade, 3rd Infantry Division. In June 1996, he assumed command of B Company, 10th Engineer Battalion (Mechanized) and held that position until October 1997. In January 1998, after completing Combined Arms Services and Staff School, he entered the Graduate School at The University of Texas at Austin. After completing his studies, CPT Sufnarski will instruct cadets in the Department of Environmental Engineering at West Point. He is married to the former Tonya Brandt of East Greenbush, New York.

Permanent Address: P.O. Box 66
                      Wells, Vermont 05774

This thesis was typed by the author.